A novel combinatorial technique for simultaneous quantification of oxygen radicals and aggregation reveals unexpected redox patterns in the activation of platelets by different physiopathological stimuli

by Dina Vara, Eugenia Cifuentes-Pagano, Patrick J. Pagano, and Giordano Pula

Title

A novel combinatorial technique for simultaneous quantification of oxygen radicals and aggregation reveals unexpected redox patterns in the activation of platelets by different physiopathological stimuli

Short Title

Redox-dependent regulation of platelets

Authors

Dina Vara[1], Eugenia Cifuentes-Pagano[2], Patrick J. Pagano[2], and Giordano Pula[1,*]

[1]Institute of Biomedical and Clinical Science, University of Exeter Medical School, Exeter, United Kingdom.
[2]Department of Pharmacology & Chemical Biology and Vascular Medicine Institute, School of Medicine, University of Pittsburgh, Pittsburgh, US

*Corresponding author: Giordano Pula, Institute of Biomedical and Clinical Sciences (IBCS), University of Exeter Medical School (UEMS), EMS Building, room F08b, St Lukes Campus, EX1 2LU, Exeter (UK), email: g.pula@exeter.ac.uk, Tel: 01392722920, Mob: 07854579804

Word counts (text): 4,642
Word counts (abstract): 243
Figure count: 8 (plus 13 supplementary)
Table count: 0
Reference count: 50

Key points:
1) We have developed a technique to measure platelet function and oxidative stress simultaneously, which will accelerate research in this field.
2) We have highlighted common patterns and key differences in redox responses to different stimuli, which may open new drug discovery opportunities

Abstract

The regulation of platelets by oxidants is critical for vascular health and may explain thrombotic complications in diseases such as diabetes and dementia, but remains poorly understood.

Here, we describe a novel technique combining electron paramagnetic resonance spectroscopy and turbidimetry, which has been utilised to monitor simultaneously platelet activation and oxygen radical generation. This technique has been used to investigate the redox-dependence of human and mouse platelets.

Using selective peptide inhibitors of NOXs on human platelets and genetically modified mouse platelets (NOX1$^{-/-}$ or NOX2$^{-/-}$), we discovered that:1) intracellular but not extracellular superoxide anion generated by NADPH oxidases (NOXs) is critical for platelet activation by collagen; 2) superoxide dismutation to hydrogen peroxide is required for thrombin-dependent activation; 3) NOX1 is the main source of oxygen radicals in response to collagen, while NOX2 is critical for activation by thrombin; 4) two platelet modulators, namely oxidised low density lipoproteins (oxLDL) and amyloid peptide β (Aβ), require activation of both NOX1 and NOX2 to pre-activate platelets.

This study provides new insights on the redox dependence of platelet activation. It suggests the possibility of selectively inhibiting platelet agonists by targeting either NOX1 (for collagen) or NOX2 (for thrombin). Selective inhibition of either NOX1 or NOX2 impairs the potentiatory effect of tested platelet modulators (oxLDL and Aβ), but does not completely abolish platelet haemostatic function. This information offers new opportunities for the development of disease specific antiplatelet drugs with limited bleeding side effects by selectively targeting one NOX isoenzyme.

Introduction

Platelets are anucleated circulating cells responsible for initiating haemostasis *via* thrombus formation and blood clotting. The regulation of platelets is of primary importance for cardiovascular medicine and for the discovery of new drugs to treat cardiovascular diseases (1). In addition to canonical signalling pathways depending on protein kinase activity (2), platelets are regulated in a redox-dependent manner. Several lines of evidence suggest that platelets are modulated by extracellular reactive oxygen species (ROS) (3) and that platelet activation is essentially dependent on the generation of endogenous ROS (4-6). Therefore, the study of platelet regulation and haemostasis is shedding light on the interface between ROS biochemistry and cellular physiology. Superoxide anion ($O_2^{\bullet-}$) from exogenous sources or endogenously produced by platelets is shown to significantly increase platelet aggregation and thrombus formation (7). $O2^{\bullet-}$ has a pre-eminent role in biology and pathophysiology, as it serves as a progenitor for formation of hydrogen peroxide (H_2O_2), peroxynitrite ($ONOO^{\bullet-}$) and hydroxyl radical ($HO^{\bullet}$), and thereby plays a key role in the post-translational oxidative modification of proteins (8). The work of several research groups has focussed on NADPH oxidases (NOXs) as important sources of ROS in platelets responsible for the regulation of platelet responsiveness (9-15). Despite the increased interest on this aspect of platelet biology and haemostasis regulation, progress within this field is hampered by the lack of reliable and quantitative techniques for the analysis of platelet oxidative state (16, 17). This has made it challenging to completely appreciate the importance of endogenous and exogenous oxidants on the regulation of platelet signalling pathways and on the balance between haemostasis and thrombosis in health and disease. Indirectly, this has impeded the development of pharmacological treatments for thrombotic conditions based on the control of ROS generation. We addressed this biomedical need by combining the measurement of platelet activation (using turbidimetry (18)) and the simultaneous measurement of intracellular or extracellular oxygen radicals (using electron paramagnetic resonance or EPR spectroscopy (19, 20)) into one multiplex technique that allows the accurate study of the oxidative state and function of human platelets.

This technique is likely to find application in clinical practice, where the simultaneous analysis of platelet responsiveness and oxidative stress can aid developing more advanced diagnostics for patients at risk of thrombotic diseases. It could also find application in drug discovery, as NOX modulation is becoming an important therapeutic strategy in several diseases (21, 22). In the cardiovascular field, in order to avoid side effects and bleeding complications of antithrombotic drugs, modern drug discovery aims to develop targeted approaches to interfere with the contribution of platelets to pathological alterations of the vascular system while preserving their vascular protective functions (23, 24). Within this context, it is imperative to deepen our understanding of the regulation of platelets in both health and disease, as redox-dependent regulation of platelets remains poorly understood (25). Our novel approach can help to clarify redox-dependent mechanisms regulating platelets and haemostasis, validate new drug discovery targets and identify novel antiplatelet drug candidates.

In this study, we utilised the EPR/turbidimetry technique to clarify the dynamics of oxygen radical generation and activation in human platelets in response to physiological and pathological stimuli. The use of NOX1- and NOX2-selective peptide inhibitors allowed for the identification of key differences in the involvement

of these two enzymes in the response to platelet agonists and modulators. The application of this technique will further our understanding of redox-dependent platelet regulation and may have important consequences for antiplatelet drug discovery, where the quest for truly pathway-specific inhibitors targeting pathological platelet activation without interfering with their physiological haemostatic function remains an unmet objective.

Methods
A detailed description of the methods is available as supplemental material available online.

Platelet preparation
Human blood was drawn from healthy volunteers by median cubital vein venepuncture following Royal Devon and Exeter NHS Foundation Trust Code of Ethics and Research Conduct and under NRES South West – Central Bristol ethics committee approval (Rec n. 14/SW/1089). Sodium citrate was used as anticoagulant (0.5% w/v). PRP was separated from whole blood by centrifugation (250 × g, 17 min), and platelets were separated from PRP by a second centrifugation step (500 × g, 10 min), in the presence of prostaglandin E1 (PGE1, 40 ng/ml) and indomethacin (10 µM).

EPR/turbidimetry assay
2×10^8 platelets/ml were prepared as described above. Prior to adding stimuli, 200 µM CMH or PPH was added to platelets. Platelet suspensions were loaded onto a Chronolog 700-2 aggregometer with continuous stirring and the turbidimetry readings were immediately started. 50 µl of platelet-free supernatant were transferred into the Hirschmann precision micropipettes and read using an e-scan (Noxygen, Germany).

Thrombus formation under physiological flow assay
The Bioflux200 system (Fluxion, South San Francisco, CA) was used to analyse thrombus formation in human and mouse whole blood under flow. Heparin-anticoagulated whole blood was incubated with scrambled or the NOX inhibitory peptides, NoxA1ds and Nox2ds-tat before the addition of 1 µM DiOC6 for 10 minutes before the blood was added to the wells. Thrombus formation was visualized by fluorescence microscopy at a shear rate of 1000 sec^{-1}

Results
Superoxide anion-dependence of platelet activation by collagen but not thrombin
Generation of ROS in a living cell can be examined by electron paramagnetic resonance (EPR) spectroscopy using 1-hydroxy-3-methoxycarbonyl-2,2,5,5-tetramethylpyrrolidine (CMH), an oxygen radical-specific spin probe (16). This spin probe crosses the plasma membrane and directly reacts with intracellular oxygen radicals to generate a nitroxide adduct that can be detected by EPR spectroscopy (Supplementary Figure 1A-B). We combined classical aggregometry (also known as turbidimetry) with CMH-dependent and EPR spectroscopy by analysing CMH oxidation in the platelet supernatant while the aggregation reaction is taking place (Supplementary Figure 1C). EPR is considered a gold standard for ROS detection and offers the important advantage of providing a quantification of the generation

4

rate of oxygen radicals. As shown in Supplementary Figure 2A-B, it is in fact possible to build a calibration curve using known concentrations of the nitroxide adduct (CM$^{\bullet}$). Knowing platelet suspension density and incubation time, it is therefore possible to interpolate experimental data of resonance intensity into CMH oxidation rates (moles per platelet per minute, using the formula shown in Supplementary Figure 2C). This assay allowed us to correlate platelet aggregation induced by collagen and thrombin with the rate of oxygen radical generation (measured as rate of CMH oxidation). Collagen was tested at concentrations ranging from 1 to 30 μg/ml and both aggregation kinetics (Figure 1A) and oxygen radical generation rates at 10 minutes from stimulus delivery (Figure 1B) were concentration-dependent. Similarly to collagen, a synthetic collagen-related peptide (CRP) that selectively engages GPVI receptor (but not other collagen-binding receptors on platelets), also led to concentration-dependent $O_2^{\bullet-}$ formation that was necessary for platelet aggregation (Supplementary Figure 3). Thrombin also showed concentration-dependence of both EPR and aggregation responses between 0.03 and 1 unit/ml (Figure 1C and D, respectively). Supplementary Table 1 shows the EC50 values of these three agonists for EPR detection of superoxide anion generation and aggregation response.

In order to confirm the chemical nature of the oxygen radicals generated by platelets upon activation and detected by EPR, we utilised cell-permeant pegylated superoxide dismutase (PEG-SOD), which scavenges $O_2^{\bullet-}$ by dismuting it into H_2O_2. The EPR signal detected in human platelets stimulated by collagen and thrombin was abolished by PEG-SOD, suggesting that $O_2^{\bullet-}$ is the oxygen radical species generated under these conditions (Supplementary Figure 4A and C, respectively). The generation of $O_2^{\bullet-}$ radicals appeared necessary for platelet activation by collagen, as the scavenging of this oxygen radical by PEG-SOD significantly inhibited aggregation in response to this agonist (Supplementary Figure 4B). On the other hand, thrombin-dependent aggregation was not affected by PEG-SOD, suggesting that $O_2^{\bullet-}$ is not an essential component of the signalling cascades induced by this agonist. Similarly to collagen, both EPR and aggregation signals in response to CRP were abolished by PEG-SOD (Supplementary Figure 3C and D). The data obtained with PEG-SOD were confirmed using another $O_2^{\bullet-}$ scavenger, 4-hydroxy-2,2,6,6-tetramethylpiperidin-1-oxyl (or TEMPOL). In Supplementary Figure 5, we show that TEMPOL abolishes the EPR signal in response to either collagen or thrombin (Supplementary Figure 5A and B, respectively), whilst only the aggregation response to collagen but not thrombin (Supplementary Figure 5C and D, respectively) is inhibited. Interestingly, the non-selective antioxidant and cell permeable amino acid N-acetyl cysteine (NAC) inhibits aggregation induced by both collagen and thrombin, suggesting that the thrombin responses depend on oxidative reactions, but that $O_2^{\bullet-}$, per se, is not the oxidant species involved in this response (Supplementary Figure 5C and D). In order to confirm that the CMH-based EPR did not detect H_2O_2 (another major ROS) in our hands, we performed experiments in the presence of catalase (CAT, non-cell permeable) and pegylated catalase (PEG-CAT, cell permeable), which convert H_2O_2 to water (Supplementary Figure 6). No effect of either enzymes on the collagen- or thrombin-induced EPR signal was observed, proving the specificity of the CMH-based EPR measurements for oxygen radicals and $O_2^{\bullet-}$ in particular.

Low levels of superoxide anion are released by platelets although they are not required for platelet activation.

We demonstrated that the CMH-based EPR spectroscopy predominantly measures intracellular but not extracellular platelet $O2^{\bullet-}$ in response to either collagen or thrombin (Supplementary Figure 7), as the non-pegylated and thus non-cell permeable version of the enzyme superoxide dismutase (SOD) did not affect the responses. Interestingly, we also utilised a non-cell permeable EPR probe called 1-Hydroxy-4-phosphono-oxy-2,2,6,6-tetramethylpiperidine (or PPH) to detect extracellular $O2^{\bullet-}$ released by platelets (Supplementary Figure 8A-D). Noticeably, the scavenging of extracellular $O2^{\bullet-}$ with SOD was effective in abolishing the PPH-based signal (Supplementary Figure 8E-F), but did not affect collagen- or thrombin-induced aggregation (Supplementary Figure 8G-H), suggesting that extracellular O2- does not participate in the process of platelet activation. In addition, we confirmed the formation of H_2O_2 in response to collagen or thrombin using the H_2O_2-specific probe Amplex Red (Supplementary Figure 9 A-B) and that catalase effectively quenched the signal. More importantly, the degradation of H_2O_2 by catalase or pegylated catalase inhibited platelet aggregation stimulated by thrombin, but not collagen (Supplementary Figure 9 C-F). This suggests that H_2O_2 is a critical component of the signalling triggered by thrombin but not collagen.

Differential role of NADPH oxidases 1 and 2 in collagen- and thrombin-dependent activation of human platelets

We utilised the combinatorial EPR/aggregometry that we developed to assess the role of NOX1 and NOX2 in platelet activation by collagen and thrombin. In experiments illustrated in Figure 5, we used the NOX1-specific inhibitory peptide NoxA1ds to assess the role of this enzyme in platelet activation (26). NOX1 inhibition almost completely inhibited oxygen radical formation in response to collagen (Figure 2A), but not thrombin (Figure 2C). In parallel, collagen- (Figure 2B) but not thrombin-dependent (Figure 2D) aggregation was inhibited by NoxA1ds. Importantly a scrambled version of the peptide was used as control. Taken together, these data suggest that NOX1 is activated and participates in the signalling of platelet activation in response to collagen but not thrombin. We also tested the role of NOX2 using the specific inhibitory peptide Nox2ds-tat (27, 28). In Figure 3, we show that both collagen- and thrombin-dependent oxygen radical formation are significantly impaired by NOX2 inhibition (Figure 3A and C, respectively). Interestingly, although the inhibition of the thrombin response by Nox2ds-tat reduces oxygen radical formation to basal levels, the inhibition of collagen-induced oxygen radical levels is only partial (i.e. in the presence of Nox2ds-tat the oxygen radical levels induced by collagen are significantly higher than resting controls). This is reflected in the aggregation data, which show complete inhibition by Nox2ds-tat of the aggregation induced by thrombin but only marginal inhibition of the response to collagen (Figure 3D and B, respectively). This is consistent with NOX1 playing a larger role than NOX2 in collagen-induced platelet aggregation. The data obtained with collagen were essentially confirmed using the synthetic ligand for GPVI CRP (Supplementary Figure 10), which suggests that GPVI is the key receptor linking collagen-dependent platelet activation to oxygen radical generation and determines the redox patterns triggered by collagen in platelets. The active engagement of NOX1 and NOX2 in collagen and thrombin signalling was confirmed by co-immunoprecipitation of these two core subunits with respective essential cytosolic components of each complex. As shown in Figure 4A, NOX1 is co-immunoprecipitated with its canonical activating subunit NOXA1 (29) in the presence of collagen, which is consistent with NOX1 being post-translationally activated in response to collagen. In Figure 4C, NOX2

appears to be co-immunoprecipitated with its canonical organizing subunit p47phox in the presence of thrombin and weakly in the presence of collagen. This aligns with the conclusions reached using our EPR and aggregation experiments, i.e. that collagen activates a primarily NOX1-dependent response, while thrombin activates primarily NOX2. Accordingly, whole blood thrombus formation experiments on collagen showed that NOX1 inhibition with NoxA1ds abolishes thrombus formation (Figure 4B), while NOX2 inhibition by Nox2ds-tat induces only a marginal inhibition (Figure 4D). Experiments in platelets from wild type, NOX1$^{-/-}$ or NOX2$^{-/-}$ mice confirmed the centrality of NOX1 for collagen signalling with marginal involvement of NOX2 in the aggregation response (Figure 5A and B), while NOX2 is critical for thrombin signalling (Figure 5C).

Role of NOX1 and NOX2 in mediating the effect on platelets of weak agonists/positive modulators oxidised LDL (oxLDL) and amyloid beta (Aβ1-42). Employing these tools (NoxA1ds (26) and Nox2ds-tat (27, 28)), we determined that NOX1 or NOX2 play an equivalent role in the generation of superoxide anion in response to oxLDL (Figure 6A) and that both enzymes are required for the stimulation of the modest aggregation induced by this modulator (Figure 6B). As suggested by the inhibition of aggregation by PEG-SOD, $O_2^{\bullet-}$ is the oxidant molecule required for the activation of platelets by oxLDL. It is important to note how oxLDL elicits a very modest aggregation (both as size and kinetic of the response), which conforms to the designation of oxLDL as a modulator rather than agonist (i.e. exerting its effect by enhancing the responsiveness of platelets to low agonist levels). In fact, low concentrations of collagen (Figure 6C) or thrombin (Figure 6D) characterised by the ability to induce no/low aggregation, resulted able to induced a robust platelet aggregation in the presence of ox-LDL. The synergistic effect of oxLDL in combination with thrombin or collagen was inhibited by NoxA1ds (Figure 6C) or Nox2ds-tat (Figure 6D), respectively. We could not test NoxA1ds on ox-LDL + collagen or Nox2ds-tat on oxLDL + thrombin, because as shown above NoxA1ds inhibits collagen directly and Nox2ds-tat inhibits thrombin directly. Similarly, Aβ1-42 induces $O_2^{\bullet-}$ formation *via* activation of NOX1 and NOX2 (Figure 7A), which leads to a modest platelet aggregation (Figure 7B). On the other hand, similarly to oxLDL, Aβ1-42 displays the ability to synergistically increase the aggregation response to low concentrations of collagen (Figure 7C) or thrombin (Figure 7D). As proved with inhibitory peptides NoxA1ds (26) and Nox2ds-tat (27, 28), the synergistic effect on collagen- or thrombin-induced aggregation is NOX1- or NOX2-dependent, respectively. We could not test NoxA1ds on Aβ1-42 + collagen or Nox2ds-tat on Aβ1-42 + thrombin, because as shown above NoxA1ds inhibits collagen directly and Nox2ds-tat inhibits thrombin directly. Transgenic mice NOX1-/- and NOX2-/- were utilised to assess the NOX-dependence of the responses to oxLDL and Aβ1-42. As ox-LDL coating of surfaces is not commonly used and there is not accepted protocol for it, we tested the effect of oxLDL added to mouse blood on thrombus formation on low levels (i.e. 0.05 mg/ml) of collagen coating (Figure 8A). These data showed that oxLDL potentiates the thrombus formation on collagen in a NOX2-dependent manner (as it was not evident in NOX2-/- blood). NOX1 ablation inhibits collagen responses directly, therefore we could not investigate the role of NOX1 in the potentiation of responses to this agonists by oxLDL. The ablation of either NOX1 or NOX2 silencing significantly also impairs thrombus formation at physiological arterial shear on absorbed Aβ1-42 (1,000 sec^{-1}) (Figure 8C), At low shear (200 sec^{-1}), mouse platelets display low levels of adhesion to absorbed Aβ1-42 without formation

of thrombi, which was inhibited by NOX1 genetic silencing but unaffected by NOX2 ablation (Supplementary Figure 11). As these modulators induce little or no aggregation on their own, we analysed the modulatory effect of oxLDL and Aβ1-42 in aggregation experiments using NOX1$^{-/-}$ and NOX2$^{-/-}$ mouse platelets. We showed that oxLDL (Figure 8B) and Aβ1-42 (Figure 8D) potentiate the aggregation induced by collagen in wild type mice but not in NOX2$^{-/-}$ mice, and the aggregation stimulated by thrombin in wild type mice but not in NOX1$^{-/-}$ mice. The potentiation of collagen response could not be tested in NOX1$^{-/-}$ mice, which do not respond to this stimulus, while the potentiation of thrombin responses could not be tested in NOX2$^{-/-}$, for the same reason.

Discussion

The study of platelet function is critical to understanding vascular homeostasis and disease. A thorough understanding of the redox-dependent regulation of platelet function has been hampered by the lack of a reliable technique to measure intracellular ROS (16, 17). We have resolved this problem by optimising an EPR-based technique for the detection of oxygen radical and combining it with a classical turbidimetric assay for the simultaneous measurement of platelet aggregation. Although EPR has been used for the analysis of ROS formation in live cells previously (16, 17), this technique has never been applied to the study of platelet redox signalling. We utilised the assay developed here to clarify several unknown aspects of the regulation of platelet activity by endogenous oxidants.

The molecular mechanisms underlying the redox dependence of platelet activation in response to collagen, thrombin, and oxidised LDL are summarised in Supplementary Figure 12. Although, the dependence of platelet activation on the generation of endogenous ROS has been described (1-6), here for the first time we elucidated the chemical nature of the ROS involved in the signalling of different platelet agonists and modulators. $O_2^{\bullet-}$ are generated in response to all tested agonists and modulators, but although these ROS are directly involved in the signalling of collagen, ox LDL and Aβ1-42, their dismutation to hydrogen peroxide is necessary for the signalling of thrombin. The literature on this aspect of platelet biology is quite inconclusive because of the use of different techniques and conditions. Although previous studies reported the generation of hydrogen peroxide in response to thrombin (and leading to apoptosis) (30), this study for the first time highlights a significant difference in the role of hydrogen peroxide in the responses to collagen and thrombin. Our observations on the link between thrombin-dependent activation and hydrogen peroxide contradict previous reports pointing to a role for hydrogen peroxide in collagen but not thrombin signalling (31). The experimental differences in our and previous studies are extensive and the poor specificity of the tools used for older studies (e.g. 2',7'–dichlorofluorescein diacetate or DCFDA) are potentially responsible for these discrepancies.

Another important addition to our understanding of redox regulation of platelets is the clarification of whether oxidants act intracellularly or extracellularly. Our data clearly suggest that platelet $O_2^{\bullet-}$ acts intracellularly in these responses, as only cell permeable scavenger can affect their activity (i.e. PEG-SOD), while hydrogen peroxide is likely to be formed by dismutation of intracellular $O_2^{\bullet-}$ and released extracellularly, where it potentiates platelet responses induced by thrombin (as proved by the effect of non-cell permeable catalase shown in supplementary Figure 6). These findings add significantly to our understanding of platelet redox regulation and are in agreement with previous suggestion of an intracellular function for $O_2^{\bullet-}$

(32, 33). It is also in agreement with the observation of a positive regulatory role for extracellular hydrogen peroxide in thrombin-induced responses (34) and a role for extracellular oxidants in the regulation of platelet surface receptor function by protein disulphide isomerases (PDIs) (35). Regarding the redox-dependence of the collagen signalling in platelets, although further studies are required, protein tyrosine phosphatases (PTPs) are the most likely link between redox and conventional signalling in platelets (36). The oxidative inactivation of protein phosphatases has in fact been suggested to play a key role in the activation and regulation of the pathophysiological roles of platelets (37). The Src Homology Phosphatase 2 (SHP2) has been shown to play an important role as a negative regulator of platelet activation (38) and recent studies demonstrated that ROS generated during platelet activation oxidise and inhibit SHP2. This, in turns, facilitates the activation of protein kinase-mediated signalling pathways and drives the processes associated with cell activation (e.g. adhesion receptor activation, shape change, etc.) (37, 39).

In this study, we also highlight the differential involvement of NOX1 and NOX2 in physiological agonist signalling (i.e. collagen and thrombin). NOX1 is essential for the signalling of collagen with NOX2 inhibition only partially reducing collagen-dependent aggregation and $O_2^{\bullet-}$ formation, in both human (Figure 3A-B) and mouse (Figure 5A) platelets. The secondary role of NOX2 in collagen responses is further demonstrated by thrombus formation experiments under physiological flow, which is marginally but significantly reduced by NOX2 inhibition/silencing in human but not mouse blood (i.e. Figure 4D vs Figure 5B). This discrepancy between thrombus formation in human and mouse blood could be suggestive of a higher involvement of NOX2 in collagen responses of human platelets. In any case, the dominant role of NOX1 in collagen response is clear in our experiments both in human and mouse platelets. Similarly, NOX2 is essential for the signalling of thrombin without NOX1 involvement in human platelets (Figure 2C-D) and limited yet significant involvement in mouse platelets (Figure 5C). This is in agreement with previous indications from our and other groups (14, 40), but in essential disagreement with a recent study in mouse platelets reaching opposite conclusions (i.e. NOX1 involvement in thrombin signalling and NOX2 involvement in Collagen signalling) (13). Some differences can be expected between signalling pathways and redox dependence of human and mouse platelets, which may explain this discrepancy. Overall, combining human and mouse platelet data, it is safe to state that thrombin-dependent aggregation depends very heavily on NOX2 activity (although a role of NOX1 in thrombin was detected in mouse platelets, which we did not observe in human platelets), while collagen-induced aggregation was predominantly NOX1-dependent with marginal involvement of NOX2 (as shown in our human platelet data). So, although mouse platelets display some engagement of NOX1 in thrombin responses, species-specific differences cannot fully explain the discrepancy between our report and Delaney's work. The fact that Delaney and colleagues used male animals for NOX1 studies and females for NOX2 studies may explain some of the differences with our study (performed entirely on female animals). Other potentially important differences are in the platelet isolation procedure, the concentration of agonists (very low concentration of thrombin used) and the use of collagen-related peptide instead of collagen.

In addition to physiological stimuli, in this study we analysed the effect of oxidised LDL and Aβ1-42, platelet modulators associated with the thrombotic complications of atherosclerosis (41) and cerebrovascular amyloid angiopathy (CAA) (42), respectively. Both oxidised LDL and Aβ1-42 have been shown to activate platelets and act as positive modulators (15, 43). We confirmed the ability of these molecules

to induce partial platelet aggregation. On the other hand, they were able to significantly increase the responses to low levels of physiological agonists. This mode of action is consistent with the definition of positive modulators or primers (44), which are characterised by the ability to trigger an unwanted haemostatic response and clot formation leading to thrombosis. The involvement of platelet positive modulators in thrombotic complications associated with diseases is particularly important for vascular health and relative pharmacotherapy (45). Interestingly, the aggregation induced by these primers was also redox-dependent and inhibited by the $O_2^{\bullet-}$ scavenger PEG-SOD. This is in agreement with previous literature on oxLDL (15, 46) and Aβ1-42 (47), and supports the hypothesis that platelet primers may act in a redox-dependent manner (48).

Also intriguing were our conclusions regarding the involvement of NOX1 and NOX2 in the signalling of oxLDL and Aβ1-42. We provide compelling evidence in human platelets with NOX-selective inhibitors Nox2ds-tat and NoxA1ds or in genetically modified mouse platelets ($NOX1^{-/-}$ or $NOX2^{-/-}$) that both NOX1 and NOX2 are activated by oxLDL and Aβ1-42 and they are both required for the functional effects of these pathology-associated modulators on platelets. These conclusions were confirmed by experiments with transgenic mouse platelets, both in thrombus adhesion and aggregation experiments. Only adhesion to Aβ1-42 under low shear seemed exclusively NOX1-dependent. This is a low level adhesion response incapable of properly triggering thrombus formation (Supplementary Figure 11). These data may therefore suggest a differential involvement of NOX1 and NOX2 in different molecular events triggered by Aβ1-42. This hypothesis would deserve further study for satisfactory elucidation. The involvement of NOX2 in the signalling of oxLDL has been suggested previously (15, 46), while the involvement of NOX1 is novel. The possibility of abolishing the effect of oxLDL and Aβ1-42 on platelets by inhibiting only one of the two NOXs may suggest that both enzymes are required for reaching a threshold in the superoxide anion levels leading to platelets stimulation. The similarities between the activity and redox-dependence of oxLDL and Aβ1-42 may suggest that they act on similar receptors. As suggested by literature for both molecules, the receptors that these platelet modulators are likely to be CD36 (15, 49). Importantly, the fact that both platelet NOXs are required for the modulatory activity of oxLDL or Aβ1-42 offers the opportunity of targeted intervention without the complete inhibition of the response to physiological agonists. In other words, the inhibition of only one NOX isozyme could reduce the pro-thrombotic tendencies associated with vascular inflammation without completely impairing the haemostatic response (i.e. NOX1 inhibition will not impair thrombin response, while NOX2 inhibition will not impair collagen responses). This is the ultimate goal of modern antiplatelet drug discovery and may help to resolve the persisting problem of bleeding risks associated with all existing antiplatelet treatment (50).

In summary, herein we describe the development and application of a novel approach to simultaneously monitor the generation of oxygen radicals and platelet aggregation. This technique has the potential to become a standard technique to assess platelet responsiveness and thrombotic risks associated to vascular conditions in a clinical setting. In addition, this study allowed the identification of patterns of platelet regulation and the clarification of the mode of action of physiological agonists and pathological modulators of platelets. The results of this study also highlight the potential of NADPH oxidase targeting for the development of novel antiplatelet drugs with better pharmacodynamic profiles (i.e. limited bleeding side effects).

Author contributions
DV performed the experiments, analysed data and revised the manuscript. ECP and PJP provided essential reagents and critically reviewed the manuscript. GP designed the research, analysed data and wrote the manuscript.

Competing interests
The authors state no competing interest.

References
1. Chaudhari K, Hamad B, Syed BA. Antithrombotic drugs market. Nat Rev Drug Discov. 2014;13(8):571-572.
2. Stegner D, Nieswandt B. Platelet receptor signaling in thrombus formation. J Mol Med (Berl). 2011;89(2):109-121.
3. Iuliano L, Colavita AR, Leo R, Pratico D, Violi F. Oxygen free radicals and platelet activation. Free Radic Biol Med. 1997;22(6):999-1006.
4. Watt J, Ewart M-A, Greig FH, Oldroyd KG, Wadsworth RM, Kennedy S. The effect of reactive oxygen species on whole blood aggregation and the endothelial cell-platelet interaction in patients with coronary heart disease. Thromb Res. 2012;130(2):210-215.
5. Freedman JE. Oxidative stress and platelets. Arterioscler Thromb Vasc Biol. 2008;28(3):s11-16.
6. Ferroni P, Vazzana N, Riondino S, Cuccurullo C, Guadagni F, Davi G. Platelet function in health and disease: from molecular mechanisms, redox considerations to novel therapeutic opportunities. Antioxid Redox Signal. 2012;17(10):1447-1485.
7. Krotz F, Sohn HY, Pohl U. Reactive oxygen species: players in the platelet game. Arterioscler Thromb Vasc Biol. 2004;24(11):1988-1996.
8. Chondrogianni N, Petropoulos I, Grimm S, et al. Protein damage, repair and proteolysis. Mol Aspects Med. 2014;35:1-71.
9. Violi F, Pignatelli P. Platelet NOX, a novel target for anti-thrombotic treatment. Thromb Haemost. 2014;111(5):817-823.
10. Bartimoccia S, Carnevale R, Sanguigni V, et al. NOX 5 is expressed in platelets from patients with chronic granulomatous disease. Thromb Haemost. 2016;116(1):198-200.
11. Krotz F, Sohn HY, Gloe T, et al. NAD(P)H oxidase-dependent platelet superoxide anion release increases platelet recruitment. Blood. 2002;100(3):917-924.
12. Begonja AJ, Gambaryan S, Geiger J, et al. Platelet NAD(P)H-oxidase-generated ROS production regulates alphaIIbbeta3-integrin activation independent of the NO/cGMP pathway. Blood. 2005;106(8):2757-2760.

13.   Delaney MK, Kim K, Estevez B, et al. Differential Roles of the NADPH-Oxidase 1 and 2 in Platelet Activation and Thrombosis. Arterioscler Thromb Vasc Biol. 2016;36(5):846-854.

14.   Vara D, Campanella M, Pula G. The novel NOX inhibitor 2-acetylphenothiazine impairs collagen-dependent thrombus formation in a GPVI-dependent manner. Br J Pharmacol. 2013;168(1):212-224.

15.   Magwenzi S, Woodward C, Wraith KS, et al. Oxidized LDL activates blood platelets through CD36/NOX2-mediated inhibition of the cGMP/protein kinase G signaling cascade. Blood. 2015;125(17):2693-2703.

16.   Dikalov SI, Harrison DG. Methods for detection of mitochondrial and cellular reactive oxygen species. Antioxid Redox Signal. 2014;20(2):372-382.

17.   Griendling KK, Touyz RM, Zweier JL, et al. Measurement of Reactive Oxygen Species, Reactive Nitrogen Species, and Redox-Dependent Signaling in the Cardiovascular System: A Scientific Statement From the American Heart Association. Circ Res. 2016;119(5):e39-75.

18.   Koltai K, Kesmarky G, Feher G, Tibold A, Toth K. Platelet Aggregometry Testing: Molecular Mechanisms, Techniques and Clinical Implications. Int J Mol Sci. 2017;18(8):1803.

19.   Davies MJ. Detection and characterisation of radicals using electron paramagnetic resonance (EPR) spin trapping and related methods. Methods. 2016;109:21-30.

20.   Hawkins CL, Davies MJ. Detection and characterisation of radicals in biological materials using EPR methodology. Biochim Biophys Acta. 2014;1840(2):708-721.

21.   Bedard K, Whitehouse S, Jaquet V. Challenges, Progresses, and Promises for Developing Future NADPH Oxidase Therapeutics. Antioxid Redox Signal. 2015;23(5):355-357.

22.   Diebold BA, Smith SM, Li Y, Lambeth JD. NOX2 As a Target for Drug Development: Indications, Possible Complications, and Progress. Antioxid Redox Signal. 2015;23(5):375-405.

23.   Pudusseri A, Shameem R, Spyropoulos AC. A new paradigm shift in antithrombotic therapy. Front Pharmacol. 2013;4:133.

24.   Wong PC, Seiffert D, Bird JE, et al. Blockade of protease-activated receptor-4 (PAR4) provides robust antithrombotic activity with low bleeding. Sci Transl Med. 2017;9(371).

25.   Pietraforte D, Vona R, Marchesi A, et al. Redox control of platelet functions in physiology and pathophysiology. Antioxid Redox Signal. 2014;21(1):177-193.

26.   Ranayhossaini DJ, Rodriguez AI, Sahoo S, et al. Selective recapitulation of conserved and nonconserved regions of putative NOXA1 protein activation domain confers isoform-specific inhibition of Nox1 oxidase and attenuation of endothelial cell migration. J Biol Chem. 2013;288(51):36437-36450.

27.   Rey FE, Cifuentes ME, Kiarash A, Quinn MT, Pagano PJ. Novel competitive inhibitor of NAD(P)H oxidase assembly attenuates vascular $O_2^{(-)}$ and systolic blood pressure in mice. Circ Res. 2001;89(5):408-414.

28. Csanyi G, Cifuentes-Pagano E, Al Ghouleh I, et al. Nox2 B-loop peptide, Nox2ds, specifically inhibits the NADPH oxidase Nox2. Free Radic Biol Med. 2011;51(6):1116-1125.

29. Valente AJ, Jamali AE, Epperson TK, Gamez MJ, Pearson DW, Clark RA. NOX1 NADPH oxidase regulation by the NOXA1 SH3 domain. Free Radic Biol Med. 2007;43(3):384-396.

30. Lopez JJ, Salido GM, Gomez-Arteta E, Rosado JA, Pariente JA. Thrombin induces apoptotic events through the generation of reactive oxygen species in human platelets. J Thromb Haemost. 2007;5(6):1283-1291.

31. Pignatelli P, Pulcinelli FM, Lenti L, Gazzaniga PP, Violi F. Hydrogen peroxide is involved in collagen-induced platelet activation. Blood. 1998;91(2):484-490.

32. Qiao J, Arthur JF, Gardiner EE, Andrews RK, Zeng L, Xu K. Regulation of platelet activation and thrombus formation by reactive oxygen species. Redox Biol. 2018;14:126-130.

33. Chlopicki S, Olszanecki R, Janiszewski M, Laurindo FRM, Panz T, Miedzobrodzki J. Functional Role of NADPH Oxidase in Activation of Platelets. Antioxid Redox Signal. 2004;6(4):691-698.

34. Redondo PC, Jardin I, Hernandez-Cruz JM, Pariente JA, Salido GM, Rosado JA. Hydrogen peroxide and peroxynitrite enhance Ca2+ mobilization and aggregation in platelets from type 2 diabetic patients. Biochem Biophys Res Commun. 2005;333(3):794-802.

35. Furie B, Flaumenhaft R. Thiol isomerases in thrombus formation. Circ Res. 2014;114(7):1162-1173.

36. Jang JY, Min JH, Wang SB, et al. Resveratrol inhibits collagen-induced platelet stimulation through suppressing NADPH oxidase and oxidative inactivation of SH2 domain-containing protein tyrosine phosphatase-2. Free Radic Biol Med. 2015;89:842-851.

37. Jang JY, Min JH, Chae YH, et al. Reactive oxygen species play a critical role in collagen-induced platelet activation via SHP-2 oxidation. Antioxid Redox Signal. 2014;20(16):2528-2540.

38. Mazharian A, Mori J, Wang YJ, et al. Megakaryocyte-specific deletion of the protein-tyrosine phosphatases Shp1 and Shp2 causes abnormal megakaryocyte development, platelet production, and function. Blood. 2013;121(20):4205-4220.

39. Wang SB, Jang JY, Chae YH, et al. Kaempferol suppresses collagen-induced platelet activation by inhibiting NADPH oxidase and protecting SHP-2 from oxidative inactivation. Free Radic Biol Med. 2015;83:41-53.

40. Walsh TG, Berndt MC, Carrim N, Cowman J, Kenny D, Metharom P. The role of Nox1 and Nox2 in GPVI-dependent platelet activation and thrombus formation. Redox Biol. 2014;2:178-186.

41. Obermayer G, Afonyushkin T, Binder CJ. Oxidized low-density lipoprotein in inflammation-driven thrombosis. J Thromb Haemost. 2018;16(3):418-428.

42. Jaunmuktane Z, Mead S, Ellis M, et al. Evidence for human transmission of amyloid-beta pathology and cerebral amyloid angiopathy. Nature. 2015;525(7568):247-250.

43.   Donner L, Falker K, Gremer L, et al. Platelets contribute to amyloid-beta aggregation in cerebral vessels through integrin alphaIIbbeta3-induced outside-in signaling and clusterin release. Sci Signal. 2016;9(429):ra52.

44.   Blair TA, Moore SF, Hers I. Circulating primers enhance platelet function and induce resistance to antiplatelet therapy. J Thromb Haemost. 2015;13(8):1479-1493.

45.   Gresele P, Falcinelli E, Momi S. Potentiation and priming of platelet activation: a potential target for antiplatelet therapy. Trends Pharmacol Sci. 2008;29(7):352-60.

46.   Carnevale R, Bartimoccia S, Nocella C, et al. LDL oxidation by platelets propagates platelet activation via an oxidative stress-mediated mechanism. Atherosclerosis. 2014;237(1):108-116.

47.   Abubaker AA, Vara D, Eggleston I, Canobbio I, Pula G. A novel flow cytometry assay using dihydroethidium as redox-sensitive probe reveals NADPH oxidase-dependent generation of superoxide anion in human platelets exposed to amyloid peptide beta. Platelets. 2017;5:1-9.

48.   Dayal S, Wilson KM, Motto DG, Miller FJ Jr., Chauhan AK, Lentz SR. Hydrogen peroxide promotes aging-related platelet hyperactivation and thrombosis. Circulation. 2013;127(12):1308-1316.

49.   Herczenik E, Bouma B, Korporaal SJ, et al. Activation of human platelets by misfolded proteins. Arterioscler Thromb Vasc Biol. 2007;27(7):1657-1665.

50.   McFadyen JD, Schaff M, Peter K. Current and future antiplatelet therapies: emphasis on preserving haemostasis. Nat Rev Cardiol. 2018;15(3):181-191.

Figure legends

Figure 1: Oxygen radical generation by platelets activated by physiological stimuli collagen and thrombin. Washed human platelets were prepared as described. Collagen was tested at concentrations ranging from 1 to 30 µg/ml, while thrombin from 0.03 to 1 unit/ml. EPR was used to measure oxygen radicals formation as CMH oxidation rates (32.7 and 37.3 attomoles per platelet per minute, respectively) **(A** and **C)** and aggregation was simultaneous assessed by turbidimetry **(B** and **D)**. For either technique, representative examples are shown in top panels, while quantification is shown in the bottom panels. Aggregation curves up to 5 minutes are shown, while EPR resonance readings were taken after 10 minutes of stimulation. Examples of EPR traces and aggregation curves are representative of 4 independent experiments. Statistical analysis was performed by one-way ANOVA with Bonferroni post-hoc test (* = p <0.05, compared to resting platelets, n=4 for A-D).

Figure 2: NOX1 is specifically involved in platelet activation by collagen but not thrombin. CMH was utilised for the detection of oxygen radicals generated by platelets. 10 µg/ml collagen (**A**) or 0.1 unit/ml thrombin (**C**) were tested. 10 µM of NoxA1ds abolished the EPR response measured in the presence of collagen. The scrambled peptide at the same concentration (scNoxA1ds) was used as a negative control. Interestingly, the inhibition of NOX1 by NoxA1ds also inhibited collagen- (**B**),

but not thrombin-dependent (**D**) platelet aggregation. Aggregation curves for up to 5 minutes are shown, while EPR resonance readings were taken after 10 minutes of stimulation. Examples of EPR traces and aggregation curves are representative of 3 or more independent experiments. Statistical analysis was performed by one-way ANOVA with Bonferroni post-hoc test for EPR (* = p <0.05, compared to resting platelets) or t test for aggregation (* = p <0.05, compared to scrambled control, n=3 for A-D).

Figure 3: NOX2 is activated by both collagen and thrombin, but essential only for platelet aggregation induced by thrombin. CMH was utilised for the detection of oxygen radicals generated by platelets. 10 µg/ml collagen (**A**) or 0.1 unit/ml thrombin (**C**) were tested. 10 µM of Nox2ds-tat inhibited the EPR response measured in the presence of either collagen or thrombin, although the collagen-dependent response remained significantly higher than resting levels of oxygen radical formation. The scrambled peptide at the same concentration (scNox2ds-tat) was used as a negative control. Interestingly, the inhibition of NOX2 by Nox2ds-tat also inhibited thrombin- (**D**), but not collagen-dependent (**B**) platelet aggregation. Examples of EPR traces and aggregation curves are representative of 3 or more independent experiments. Statistical analysis was performed by one-way ANOVA with Bonferroni post-hoc test for EPR (* = p <0.05, compared to resting platelets) or t test for aggregation (* = p <0.05, compared to scrambled control) n=4 for C and D, n=5 for A and n=7 for B).

Figure 4: NOX1 is the main source of superoxide anions in human platelet response to collagen, while NOX2 is the main source of thrombin-dependent ROS. The activation of NOX1 (**A**) and NOX2 (**B**) was assessed by co-immunoprecipitation with their canonical activating and organising subunits NOXA1 and p47^{phox}, respectively. 400 µl of platelet suspension (4 x 10^8 platelets/ml) were stimulated with 10 µg/ml collagen or 0.1 unit/ml thrombin or vehicle solution (Tyrode's buffer) for 10 minutes before gentle cell lysis (NP40 buffer). Specific NOX1 or NOX2 antibodies and Protein A/G were used to immunoprecipitate the NOX complexes (which by extension should include their regulatory subunits after activation). The immunoprecipitates were tested by immunoblotting using NOX1, NOXA1, NOX2 or p47phox antibodies (as indicated). The data are representative of 4 independent experiments. The functional role of NOX1 and NOX2 in collagen-dependent platelet activation was assessed in a whole blood flow assay (**C** and **D**). Platelets were stained with DiOC6 as described and the Bioflux platform (Fluxion, 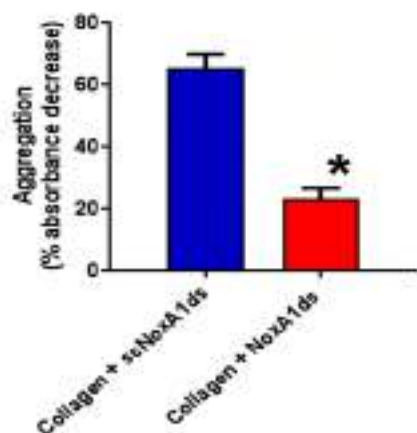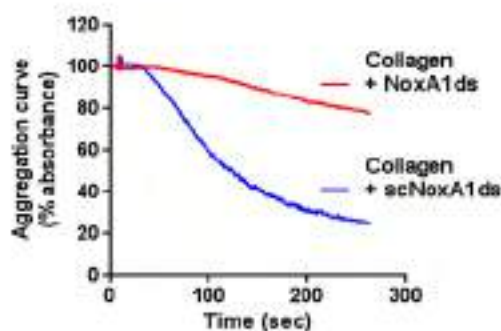San Francisco) was utilised to assess the thrombus formation induced by collagen under physiological flow (1000 sec-1). The experiments were performed in the presence of NoxA1ds or its negative scrambled control (**C**) or Nox2ds-tat or its negative scrambled control (**D**). Images were taken at 10 minutes of flow and are representative of 4 independent experiments. They were quantified by assessing the surface area coverage by platelets (lower section of panels **C** and **D**). Statistical significance was tested by t test (* = p <0.05, compared to scrambled control, n=4 for B and D).

Figure 5. NOX1- and NOX2-dependence of collagen and thrombin aggregation and superoxide generation tested in transgenic mice. Platelets were isolated for wild type (C57BL6/J), NOX1-/- or NOX2-/- mice exsanguinated via intracardiac puncture and resuspended at 2×108 platelets/ml density. Platelets were stimulated

with 3 µg/ml collagen (A) or 0.1 unit/ml thrombin (C). Aggregation (left panels) and superoxide anion formation (right panels) were measured as described for 5 and 10 minutes respectively. (B) The functional role of NOX1 and NOX2 in collagen-dependent platelet activation was also assessed in a whole blood flow assay. Platelets were stained with DiOC6 and the Bioflux platform (Fluxion, San Francisco) was utilised to assess the thrombus formation induced by collagen under physiological flow (1,000 sec-1). Images were taken at 10 minutes of flow and are representative of 4 independent experiments. They were quantified by assessing the surface area coverage by platelets with Image J. Data are representative of 4 independent experiments. Statistical analysis was performed by one-way ANOVA with Bonferroni post-hoc test (* = p <0.05, n=4 for A-C).

Figure 6: NOX1 and NOX2 are required for the induction of superoxide anion formation and platelets activation by oxidised LDL. Oxygen radical generation (**A**) and platelet aggregation (**B**) in response to oxLDL were measured as described. 10µM of scrambled NoxA1ds (scNoxA1ds), NoxA1ds, scrambled Nox2ds-tat (scNox2ds-tat), Nox2ds-tat or 100 unit/ml of PEG-SOD were pre-incubated 10 minutes before platelet stimulation with 50 ng/ml oxidised LDL (oxLDL). Examples of EPR traces and aggregation curves are representative of 4 independent experiments. Statistical analysis was performed by one-way ANOVA with Bonferroni post-hoc test (* = p <0.05, n=3 for B and n=4 for A). The effect of oxLDL as platelet modulator was investigated by traditional aggregometry (**C** and **D**). Pre-incubation with 50 ng/ml oxLDL for 10 minutes was followed by stimulation with 3µg/ml collagen (**C**) or 0.03 unit/ml thrombin (**D**). In order to test the dependence of the modulatory effect of oxLDL on NOX1 and NOX2, 10 µM scrambled NoxA1ds (scNoxA1ds), NoxA1ds, scrambled Nox2ds-tat (scNox2ds-tat), Nox2ds-tat were pre-incubated (10 minutes before addition of oxLDL). Aggregation curves are representative of 4 independent experiments.

Figure 7: NOX1 and NOX2 are required for the induction of superoxide anion formation and platelets activation by amyloid peptide β 1-42. Oxygen radical generation (**A**) and platelet aggregation (**B**) in response to amyloid peptide β 1-42 (Aβ1-42) were measured as described. 10µM of scrambled NoxA1ds (scNoxA1ds), NoxA1ds, scrambled Nox2ds-tat (scNox2ds-tat), Nox2ds-tat or 100 unit/ml of PEG-SOD were pre-incubated 10 minutes before platelet stimulation with 20µM Aβ1-42. Examples of EPR traces and aggregation curves are representative of 4 independent experiments. Statistical analysis was performed by one-way ANOVA with Bonferroni post-hoc test (* = p <0.05, n=3 for A and B). The effect of Aβ1-42 as platelet modulator was investigated by traditional aggregometry (**C** and **D**). Pre-incubation with 20µM Aβ1-42 for 10 minutes was followed by stimulation with 3µg/ml collagen (**C**) or 0.03 unit/ml thrombin (**D**). In order to test the dependence of the modulatory effect of Aβ1-42 on NOX1 and NOX2, 10 µM scrambled NoxA1ds (scNoxA1ds), NoxA1ds, scrambled Nox2ds-tat (scNox2ds-tat), Nox2ds-tat were pre-incubated (10 minutes before addition of Aβ1-42). Aggregation curves are representative of 4 independent experiments.

Figure 8: Experiments on transgenic mice suggest that NOX1 and NOX2 are required for the effect of amyloid peptide β 1-42 and oxidised LDL. Platelets from wild type, NOX1$^{-/-}$ or NOX2$^{-/-}$ mice were stained with DiOC6 and the Bioflux platform (Fluxion, San Francisco) was utilised to assess the thrombus formation

induced by collagen under physiological flow. In **A**, Ibidi Vena8+ flow chambers were coated with 0.05mg/ml collagen and whole blood was treated with 50 ng/ml native LDL (nLDL) or oxidised LDL (oxLDL). In **C**, Ibidi Vena8+ flow chambers were coated with 20µM Aβ1-42 or scrambled control peptide (ScAβ1-42). The shear rate utilised was either 1,000 sec^{-1}, which leads to thrombus formation. Images were taken at 10 minutes of flow and are representative of 4 independent experiments. They were quantified by assessing the surface area coverage by platelets with Image J. Data are representative of 4 independent experiments. Statistical analysis was performed by one-way ANOVA with Bonferroni post-hoc test (* = p <0.05, n=4 for A and C). Aggregation experiments were performed by pre-treating platelets with 50 ng/ml native LDL (nLDL) or oxidised LDL (oxLDL) (**B**) or 20µM Aβ1-42 or scrambled control peptide (ScAβ1-42) (**D**) for 10 minutes. Low level aggregation was then stimulated with either 10µg/ml collagen or 0.03 unit/ml thrombin, as indicated. Aggregation data are representative of 3 independent experiments.
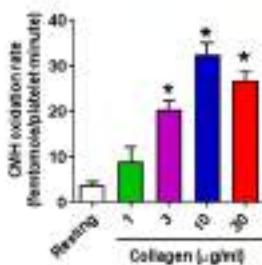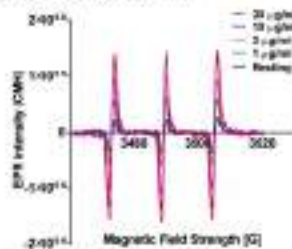
Figure 1

Figure 2

A Collagen + NOX2 inhibitor, EPR

B Collagen + NOX2 inhibitor, Aggregometry

C Thrombin + NOX2 inhibitor, EPR

D Thrombin + NOX2 inhibitor, Aggregometry

Figure 3

A NOX1 immunoprecipitation

IB: NOX1

IB: NOXA1

C NOX2 immunoprecipitation

IB: NOX2

IB: p47phox
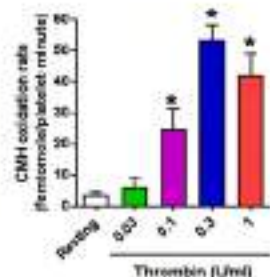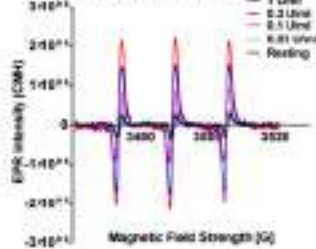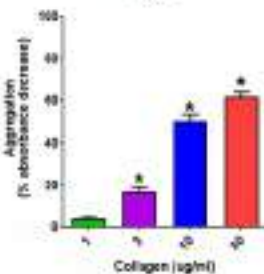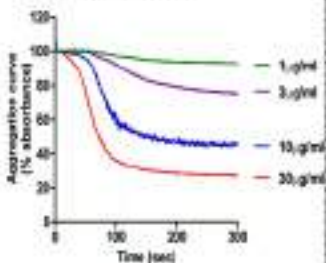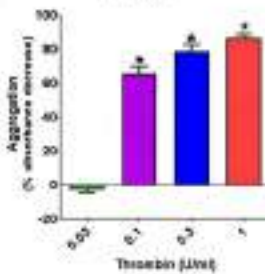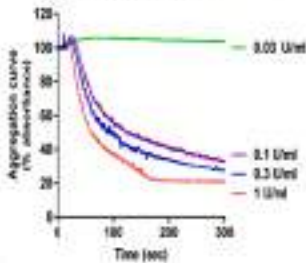
B Collagen + NOX1 inhibitor,
Flow assay

scNoxA1ds

NoxA1ds

D Collagen + NOX2 inhibitor,
Flow assay

scNox2ds-tat

Nox2ds-tat
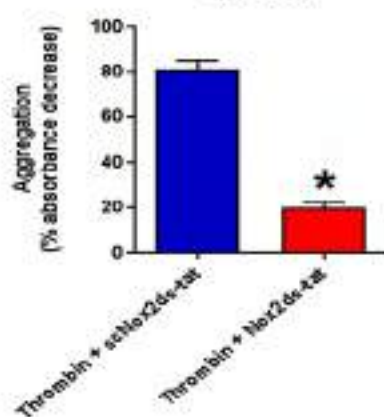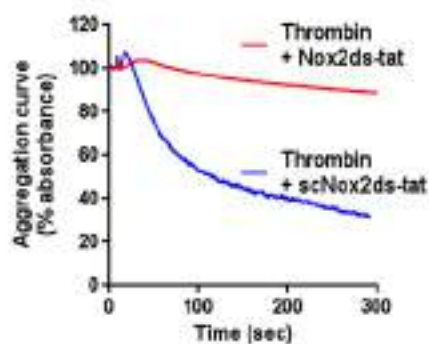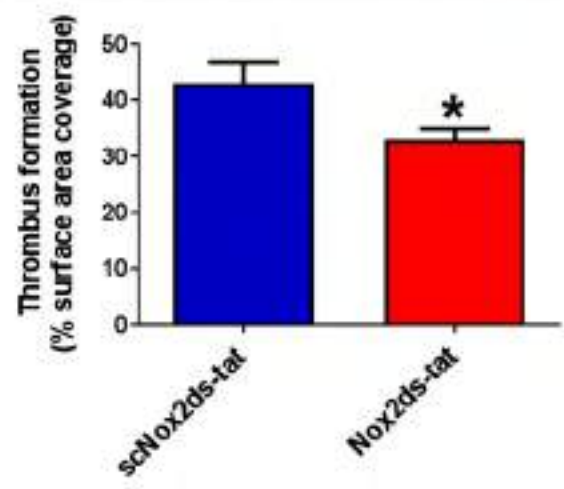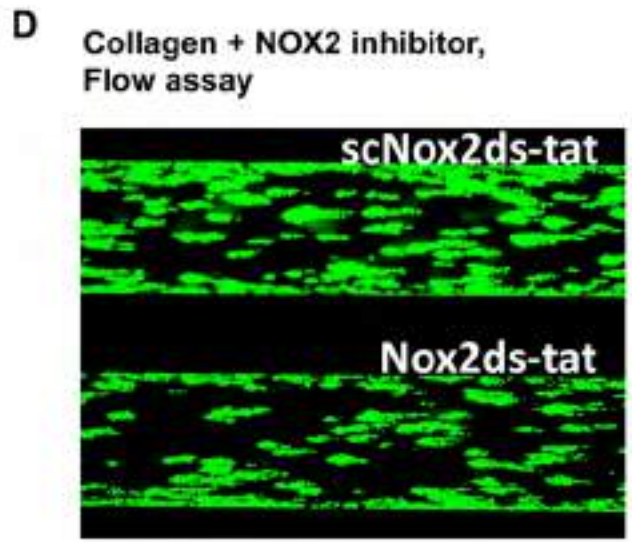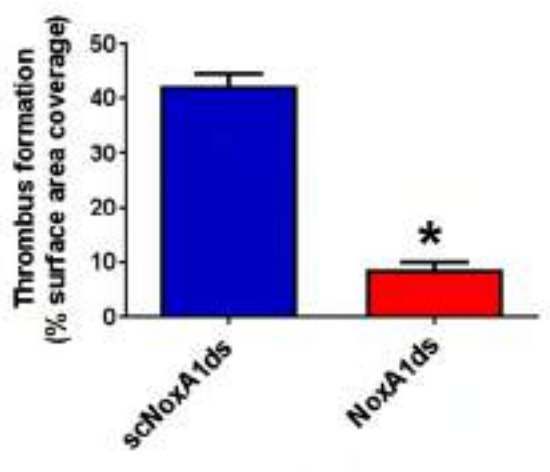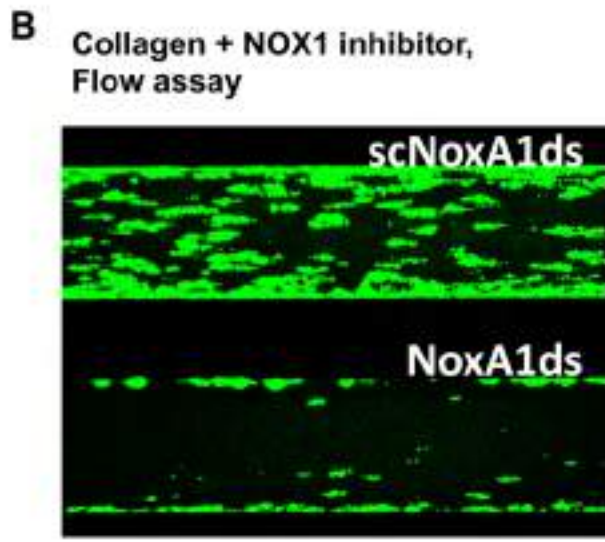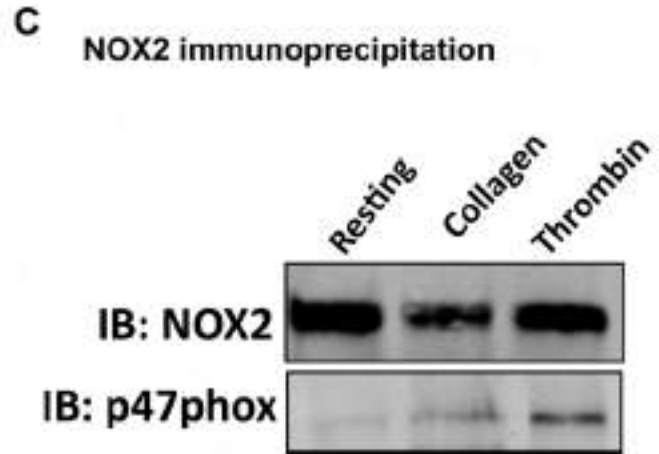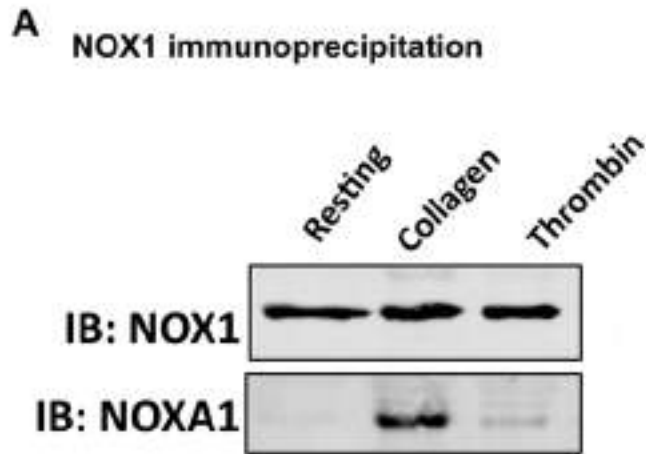
Figure 4

A Collagen
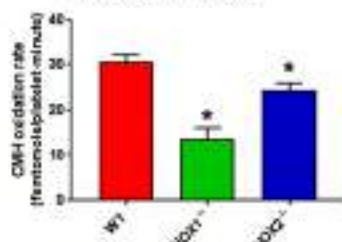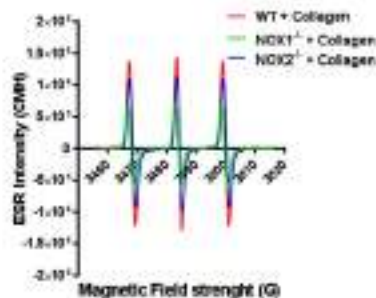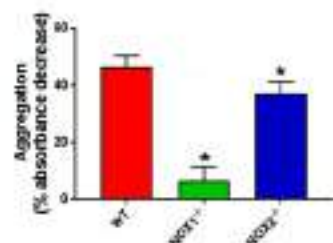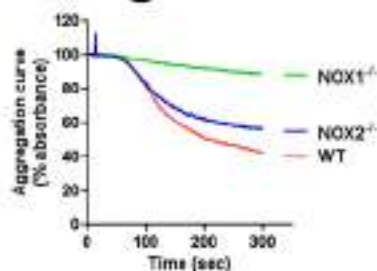
B Collagen
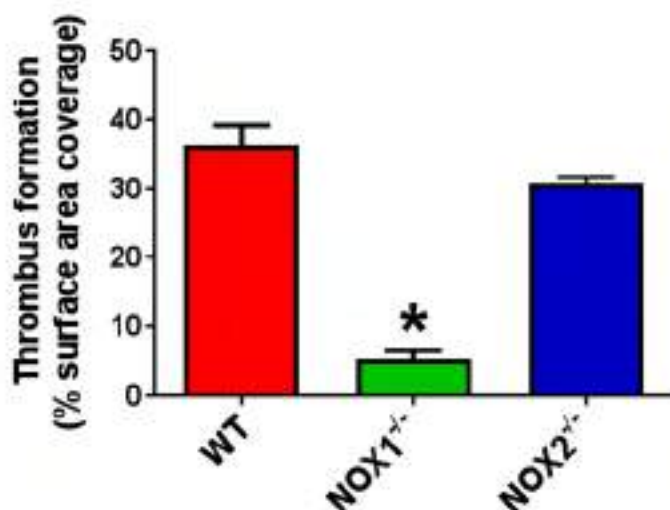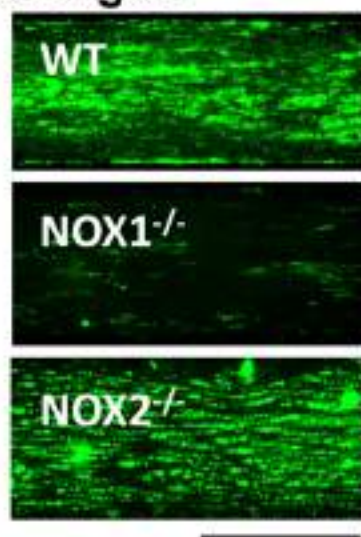
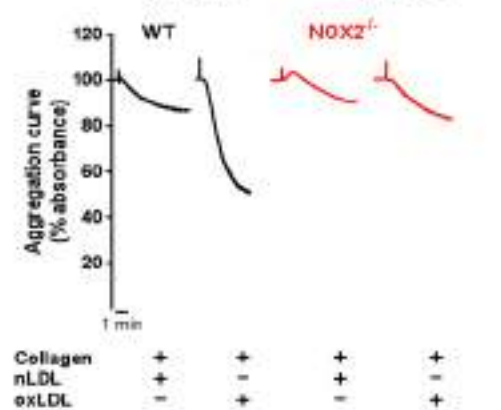
C Thrombin
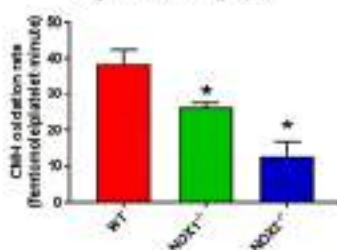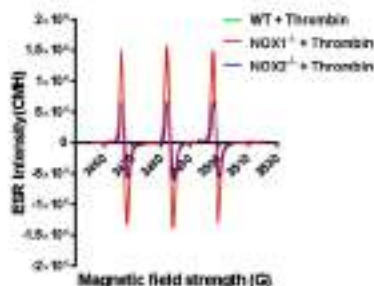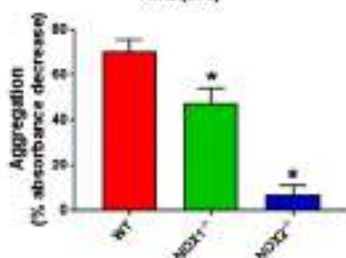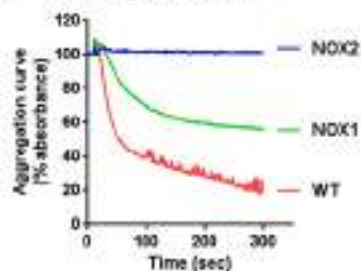
Figure 5
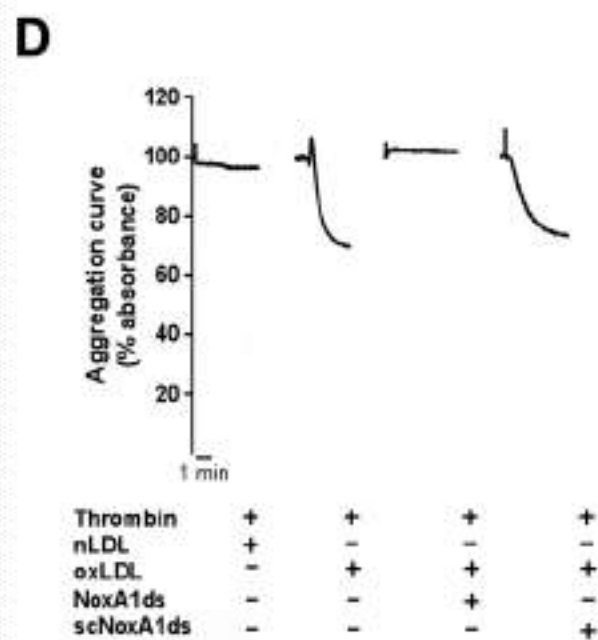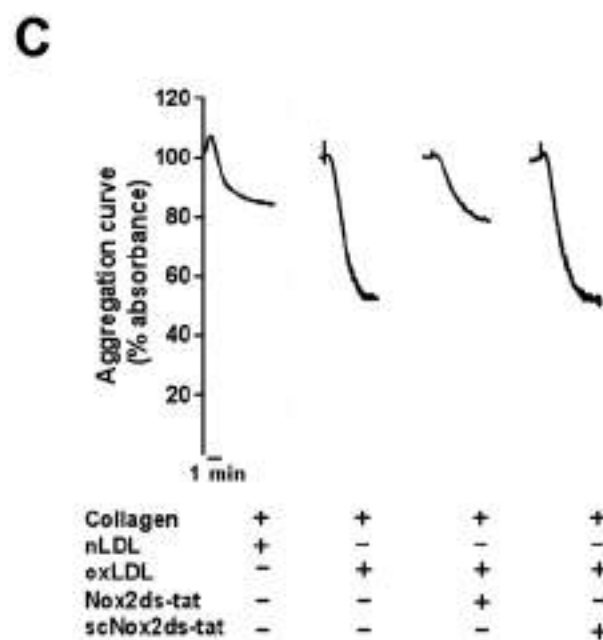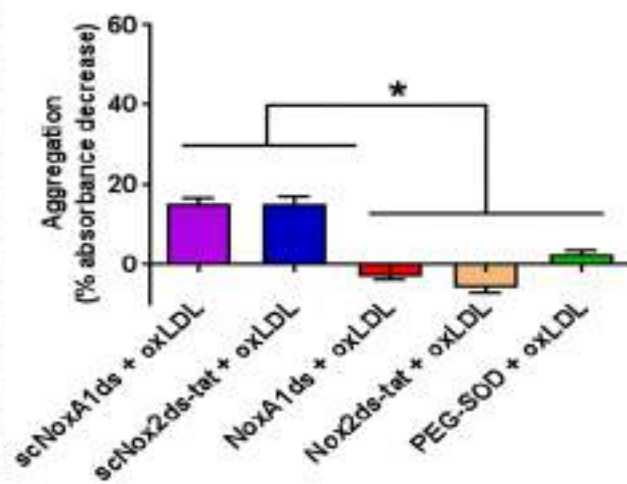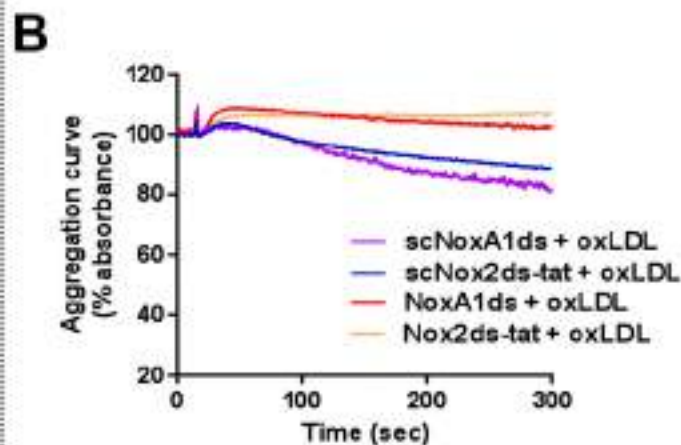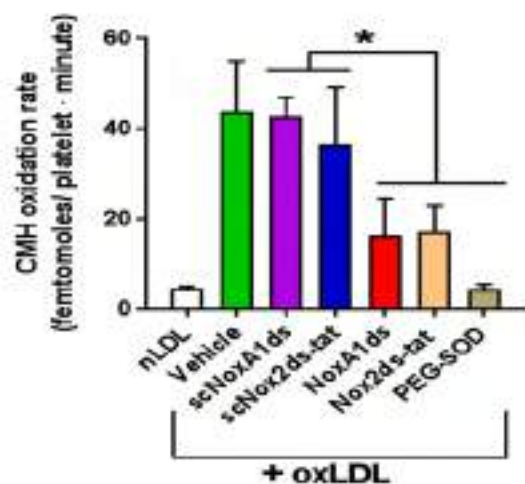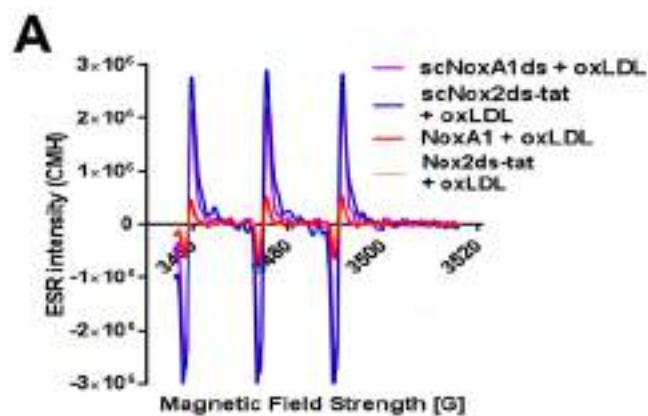
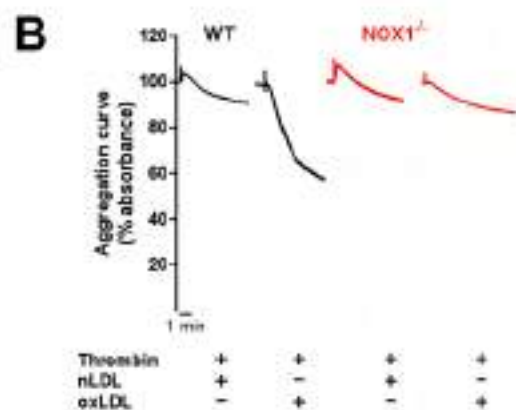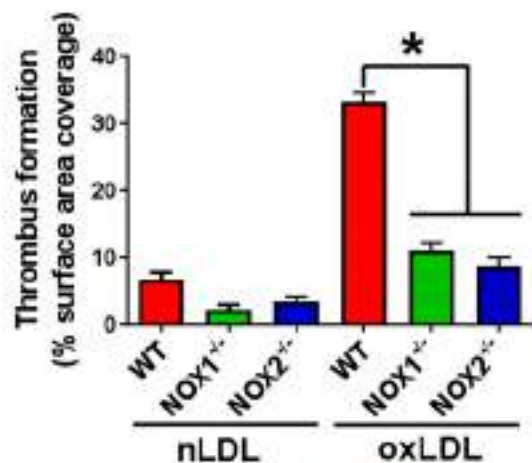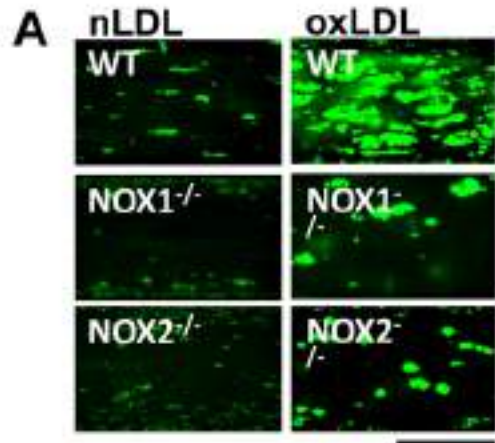**Figure 6**
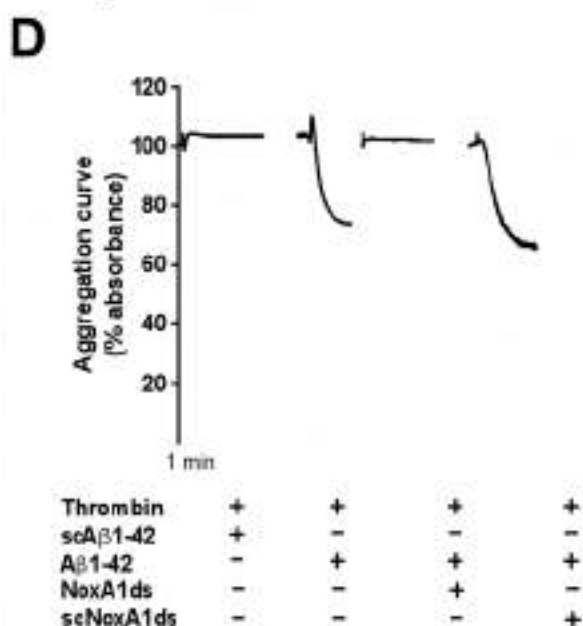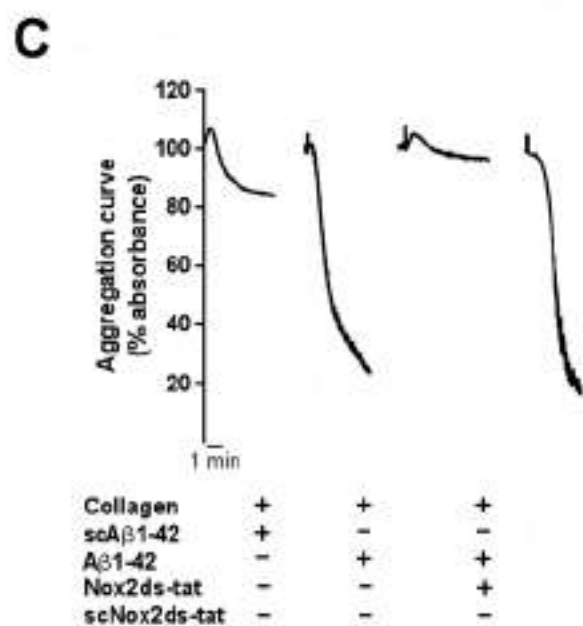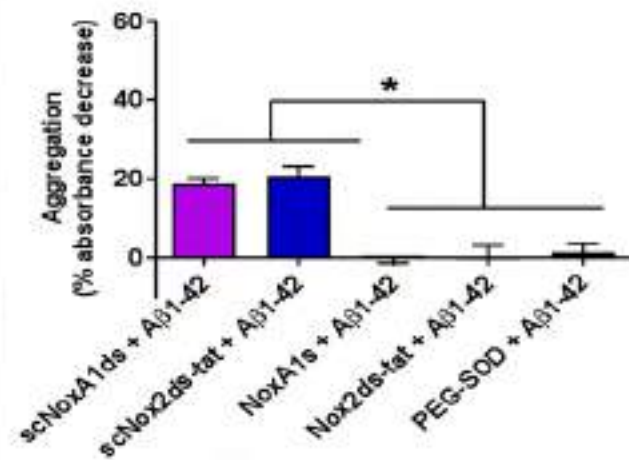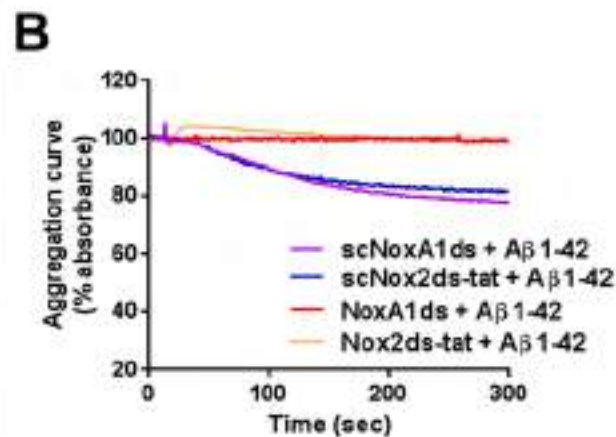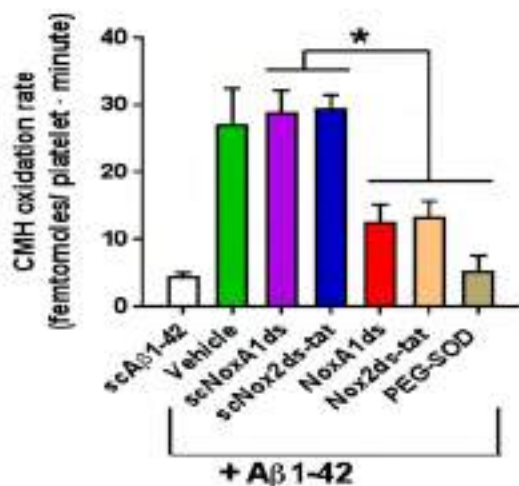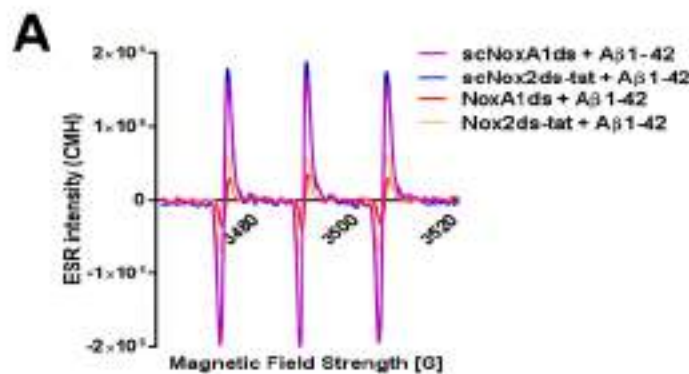
Figure 7
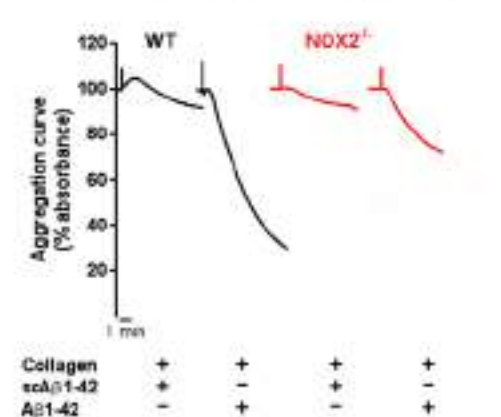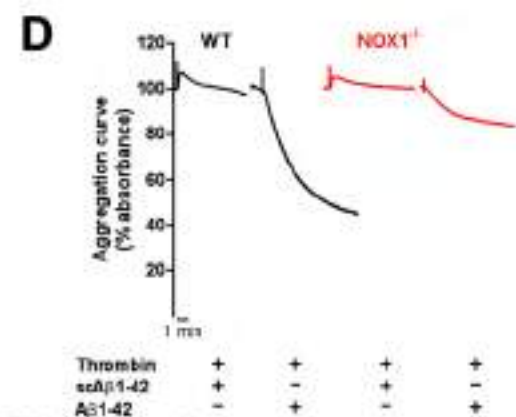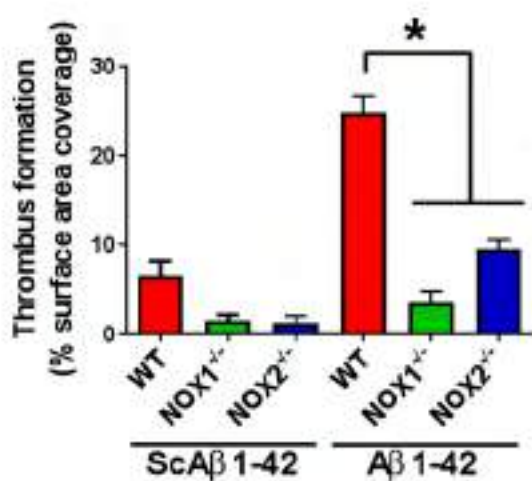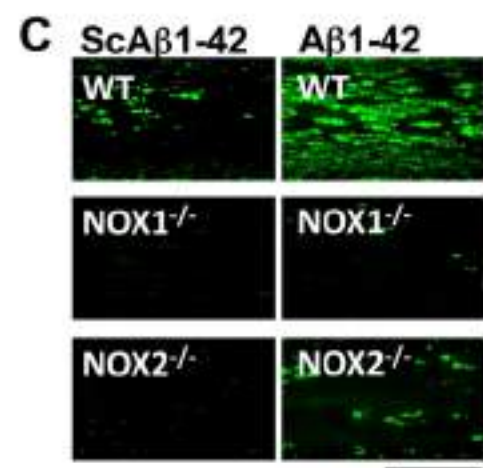
Figure 8

Online supplement

Supplemental Methods Section

Chemicals and reagents
Cyclic hydroxylamines 1-hydroxy-3-methoxycarbonyl-2,2,5,5-tetramethylpyrrolidine (CMH) and 1-hydroxy-4-phosphono-oxy-2,2,6,6-tetramethylpiperidine (PPH) were purchased from Noxygen (Elzach, Germany). Prostaglandin E1 (PGE1), indomethacin, superoxide dismutase (SOD), polyethylene glycol-conjugated superoxide dismutase (PEG-SOD), catalase (CAT), polyethylene glycol-conjugated catalase (PEG-CAT), N-acetylcysteine, 4-hydroxy-2,2,6,6-tetramethylpiperidin-1-oxyl (or TEMPOL), heparin and thrombin were obtained from Sigma-Aldrich (Poole, UK). Stock solutions of cyclic hydroxylamines (10 mM) were prepared in EPR grade Tyrode's-HEPES buffer (THB) containing 25 µM deferoxamine methanesulfonate salt (DF) and 5 µM sodium diethyldithiocarbamate trihydrate (DETC) purchased from Noxygen, (Elzach, Germany). Stock solutions were kept under argon on ice to keep an oxygen free atmosphere and were prepared daily. Native LDL (nLDL) and oxidised LDL (oxLDL) were purchased from BioRad (Oxford, UK). Horm collagen was from Nycomed (Linz, Austria). The NOX inhibitory peptides were obtained from Prof J Pagano: Nox2ds-tat (YGRKKRRQRRRCSTRIRRQL), scNox2ds-tat (RKKRRQRRRCLRITRQSR), NoxA1ds (EPVDALGKAKV) and scNoxA1ds (LVKGPDAEKVA).

Platelet preparation
Human blood was drawn from healthy volunteers by median cubital vein venepuncture under local ethics committee approval. Sodium citrate was used as anticoagulant (0.5% w/v). PRP was separated from whole blood by centrifugation (250 × g, 17 min), and platelets were separated from PRP by a second centrifugation step (500 × g, 10 min), in the presence of prostaglandin E1 (PGE1, 40 ng/ml) and indomethacin (10 µM). Washed platelets were then resuspended in a modified THB with a pH 7.4 (10 mM HEPES, 145 mM NaCl, 2.9 mM KCl, 1 mM MgCl2, 5 mM glucose, in ESR grade water (NOX-07, Noxygen, Germany) at a density of 2×10^8/ml.

EPR/turbidimetry assay
2×10^8 platelets/ml were prepared as described in the supplemental methods section. Prior to adding stimuli, 200 µM CMH or PPH was added to platelets. Platelet suspensions were loaded onto a Chronolog 700-2 aggregometer with continuous stirring (1,200rpm at 37°C) and the turbidimetry readings were immediately started. After 1 minute, stimuli were delivered and aggregation was measured for 10 minutes. After 10 min of aggregation (as determined to optimise the signal-to-noise and reproducibility of the assay), 50 µl of platelet-free supernatant were transferred into the Hirschmann precision micropipettes and read using an e-scan (Noxygen, Germany). EPR spectra were recorded using the following EPR settings: field sweep, 80 G; microwave frequency, 9.39 GHz; microwave power, 2 mW; modulation amplitude, 5 G; conversion time, 327.68 ms; time constant, 5242.88 ms; 512 points resolution and receiver gain, 1×10^4. Samples for calibration curves was obtained from a 10 mM stock solution of a standard CM$^•$ solved in THB, and diluted to concentrations of typically 0, 0.3, 1, 3, 10, and 30 µM. Exactly 50 µL of the calibration samples was transferred to Hirschmann precision micropipettes. EPR signal from samples was utilised to calculate CMH oxidation rate as described in Figure 2. The

aggregation shown in the figures span for only 5 minutes, which is sufficient for a plateau to be reached and differences in the aggregation responses to be evident. Aggregation was quantified as % absorbance decrease = (initial absorbance − final absorbance) / initial absorbance. EPR was quantified as CMH oxidation, which was obtained using a calibration curve for known concentrations of oxidised CMH (CM$^•$) (Supplementary Figure 2B) and the formula below:

$$\text{CMH oxidation rate} = \frac{[CM^•] \ x \ \text{Volume}}{\text{Platelet density x Volume x Time}}$$

Thrombus formation under physiological flow assay

The Bioflux200 system (Fluxion, South San Francisco, CA) was used to analyse thrombus formation in human and mouse whole blood under flow. Microchannels were coated with 0.1/0.05 mg·mL−1 collagen I (monomeric collagen from calf skin, Sigma, UK) for 1–2 hours at 37°C before blocking with 1% BSA in Tyrode's-HEPES buffer and washing with Tyrode's-HEPES buffer. Heparin-anticoagulated whole blood was incubated with scrambled or the NOX inhibitory peptides, NoxA1ds and Nox2ds-tat before the addition of 1 µM DiOC6 for 10 minutes before the blood was added to the wells. Thrombus formation was visualized by fluorescence microscopy at a shear rate of 200 or 1,000 sec^{-1}. Representative pictures were taken at 10 min and surface area coverage was determined using Image J.

Immunoprecipitation and pull-down assay

After stimulation, platelet were lysed under milder condition using a gentle lysis buffer (Tris 50 mM, NaCl 200 mM, Nonidet P-40 1%, Na deoxycholate 0.5%, and pH 7.4) with protease and phosphatase inhibitors. NOX1 or NOX2 was immunoprecipitated with 1 µg of rabbit mAb (Novus and Abcam respectively) overnight at 4 °C and the immunocomplexes were precipitated by addition of protein A/G Plus Agarose beads for 2 hours at 4 °C. Following brief centrifugation, immunocomplexes were washed five times with 1 ml of lysis buffer, and finally resuspended in 100 µl of SDS sample buffer 2X. Protein complexes were then analysed by Western blotting.
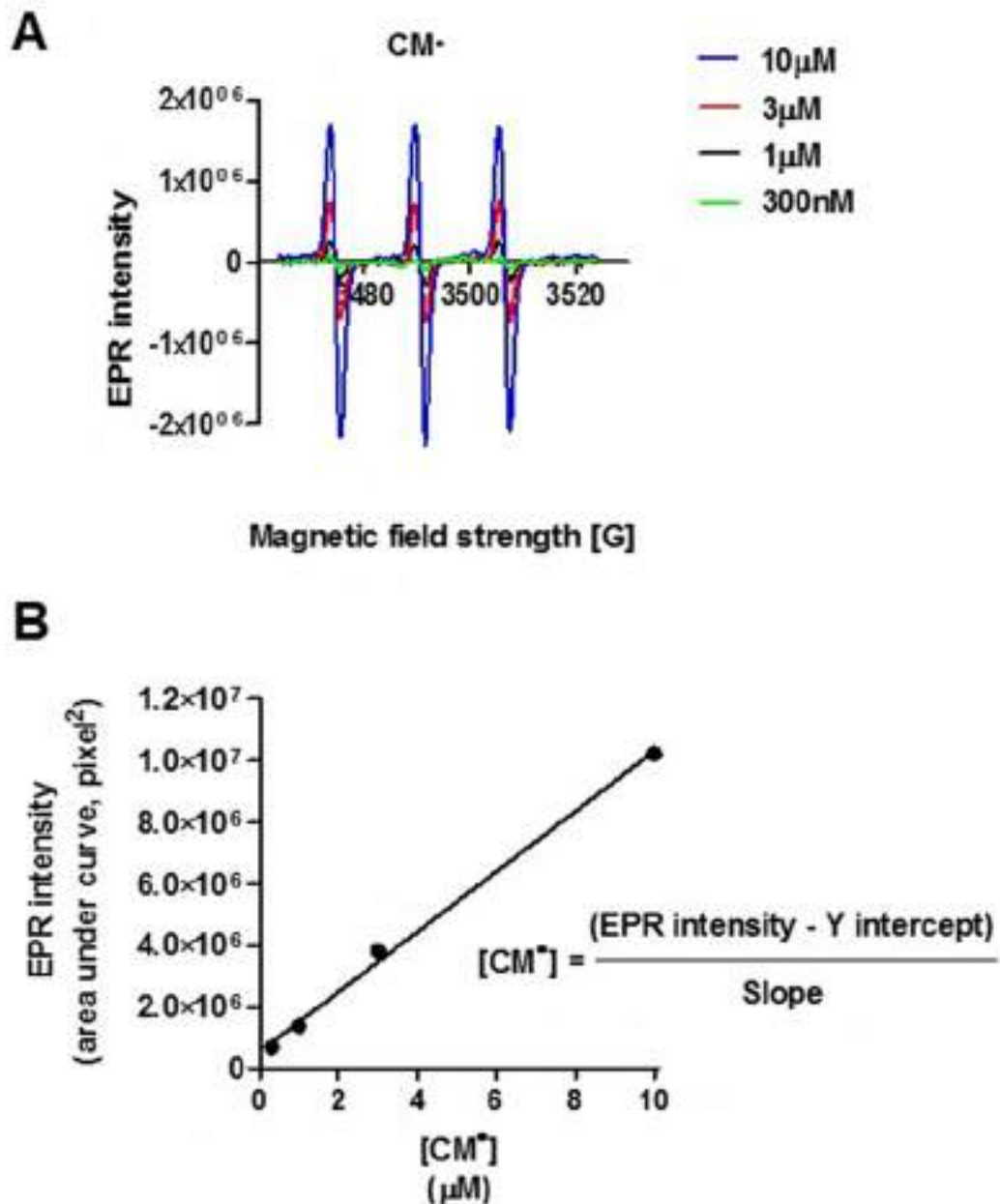
Immunoprecipitates were subjected to sodium dodecyl sulphate–polyacrylamide gel electrophoresis (SDS-PAGE) and transferred to polyvinylidene difluoride (PVDF) for immunoblotting. After blocking with blocking buffer (Odyssey® Blocking Buffer LI-COR), the corresponding PVDF membranes were incubated with anti-NOX1 goat polyclonal antibody (Sigma-Aldrich) with anti-NOXA1 mouse polyclonal antibody (Abcam) or anti-NOX2 goat polyclonal with anti-p47phox mouse monoclonal antibody (Santa Cruz, USA) overnight at 4 °C. The PVDF membranes were washed three times with wash buffer (150 mM NaCl, 10 mM Tris–HCl, pH 7.0, and 0.05 % Tween 20) and then incubated with secondary antibodies (1:15,000) for 1 hour, washed with wash buffer, and imaged on the Odyssey Clx. Secondary antibodies were produced in goat and mouse to the species of the primary antibody and were conjugated with IRdye fluorophores visible in the 700 and 800 channels of the CLx imager. Images were acquired on the CLx imager at 169 µm resolution and all processed images were free of pixel saturation.

Statistical analysis

We utilised the statistical software Graphpad Prism 7 for Windows (version 7.03, February 20th 2017). For dual comparisons we utilised t-test, while for multiple comparisons we used either Analysis Of Variance (ANOVA) plus multiple comparison post-tests (such as Bonferroni's or Tukey's test) or Non Parametric Tests such as Kruskal-Wallis. The decision on whether using ANOVA or non-parametric tests was based on the analysis of data normality (Kolmogorov-Smirnov's test) and homoscedasticity (Bartlett's test). Results were expressed as the mean + standard error (SEM) throughout the manuscript. Differences were considered significant at $p < 0.05$.
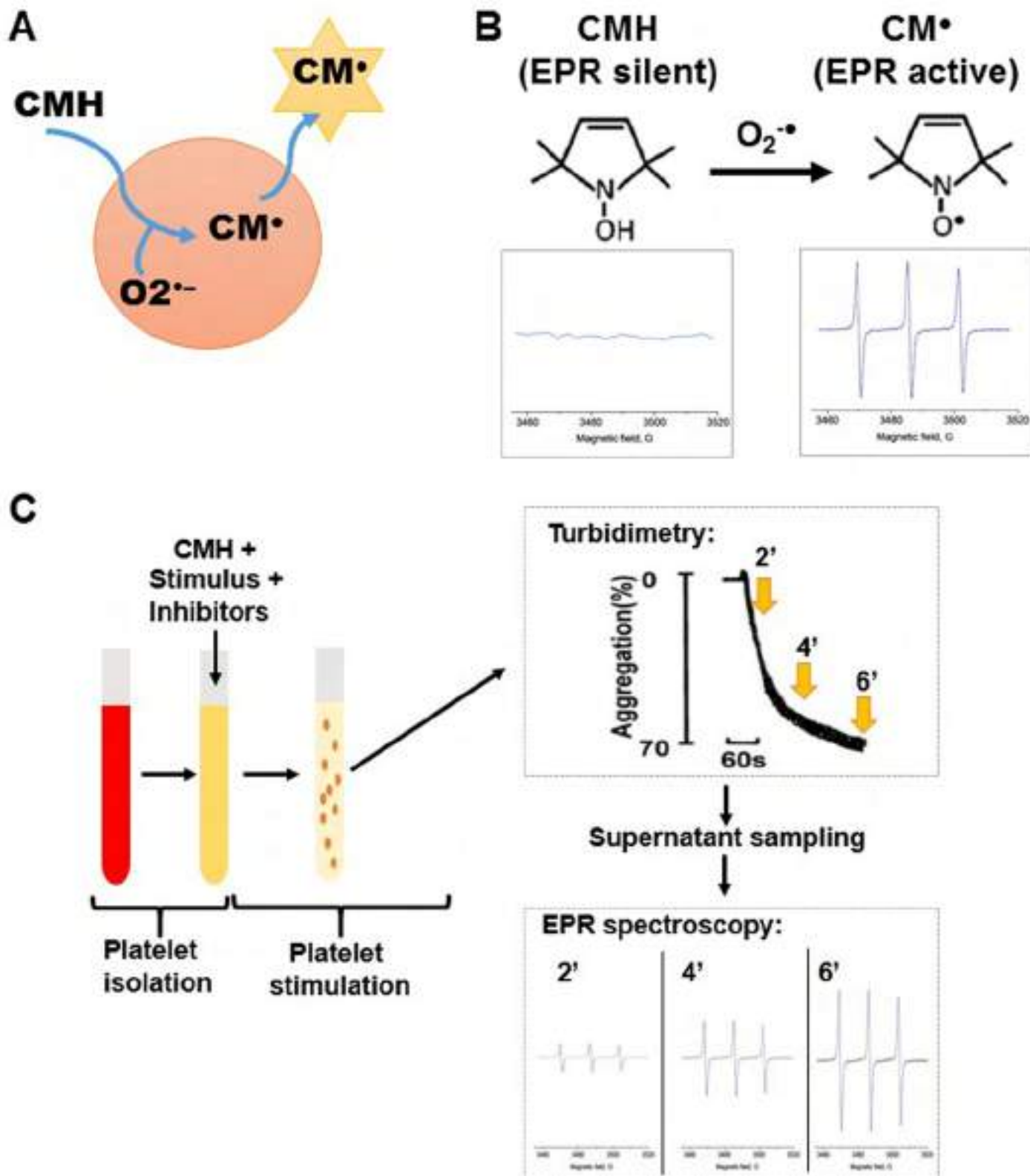
Supplementary Figure 1: Schematic diagram of the EPR/turbidimetry technique for the detection of oxygen radical generation and activation in human platelets. (A) CMH oxidation (predominantly intracellular) into CM•. (B) Chemical structure and EPR properties of CMH and CM•. (C) Schematics of the assay, with platelet isolation from whole blood, stimulation in the presence of CMH, classical turbidimetry and simultaneous EPR analysis of platelet supernatant for CMH oxidation by EPR.

A CM·

EPR intensity vs Magnetic field strength [G]

Legend: 10μM, 3μM, 1μM, 300nM

B

EPR intensity (area under curve, pixel^2) vs [CM·] (μM)

$$[CM^{\bullet}] = \frac{(EPR\ intensity - Y\ intercept)}{Slope}$$

Supplementary Figure 2: Calibration curve and CMH oxidation rate calculations. (A) Representative example of the concentration response curve for CM· (300nM to 10μM). (B) Calibration curve EPR intensity vs CM· concentration.
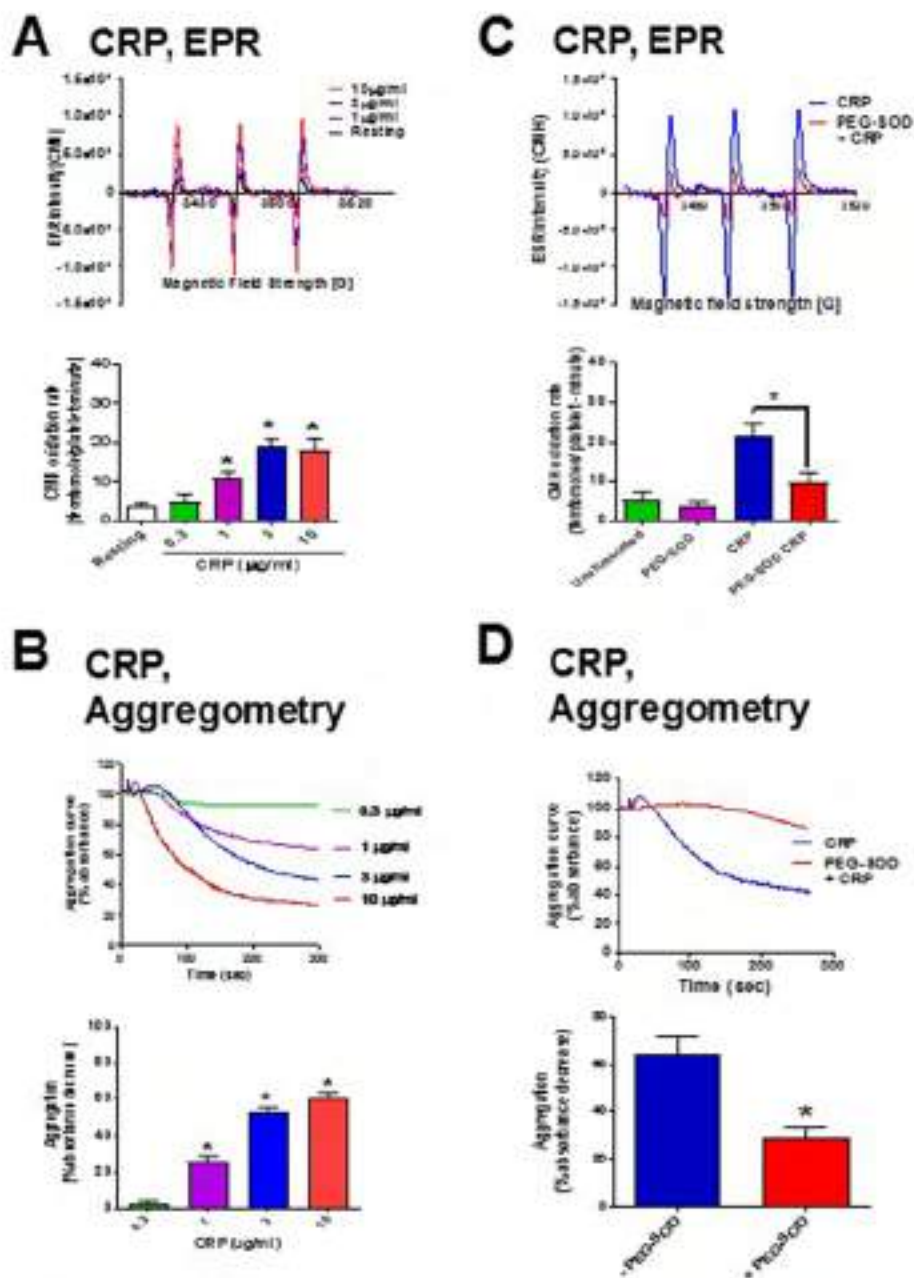
Supplementary Figure 3. CRP induced concentration-dependent increases in aggregation and oxygen radical generation rates between 0.3 and 10 µg/ml (A and B, respectively), while treatment with PEG-SOD abolished the EPR response (C) (suggesting superoxide anions are formed) and inhibited platelet aggregation (D) (which is therefore, superoxide anion-dependent). Examples of EPR traces and aggregation curves are representative of 3 independent experiments. Statistical analysis was performed by one-was ANOVA with Bonferroni post-test (A, B and C) or t-test (D). * = p <0.05, compared to resting platelets (A and B, n=3) or negative control (i.e. scrambled peptide) (C and D, n=3).
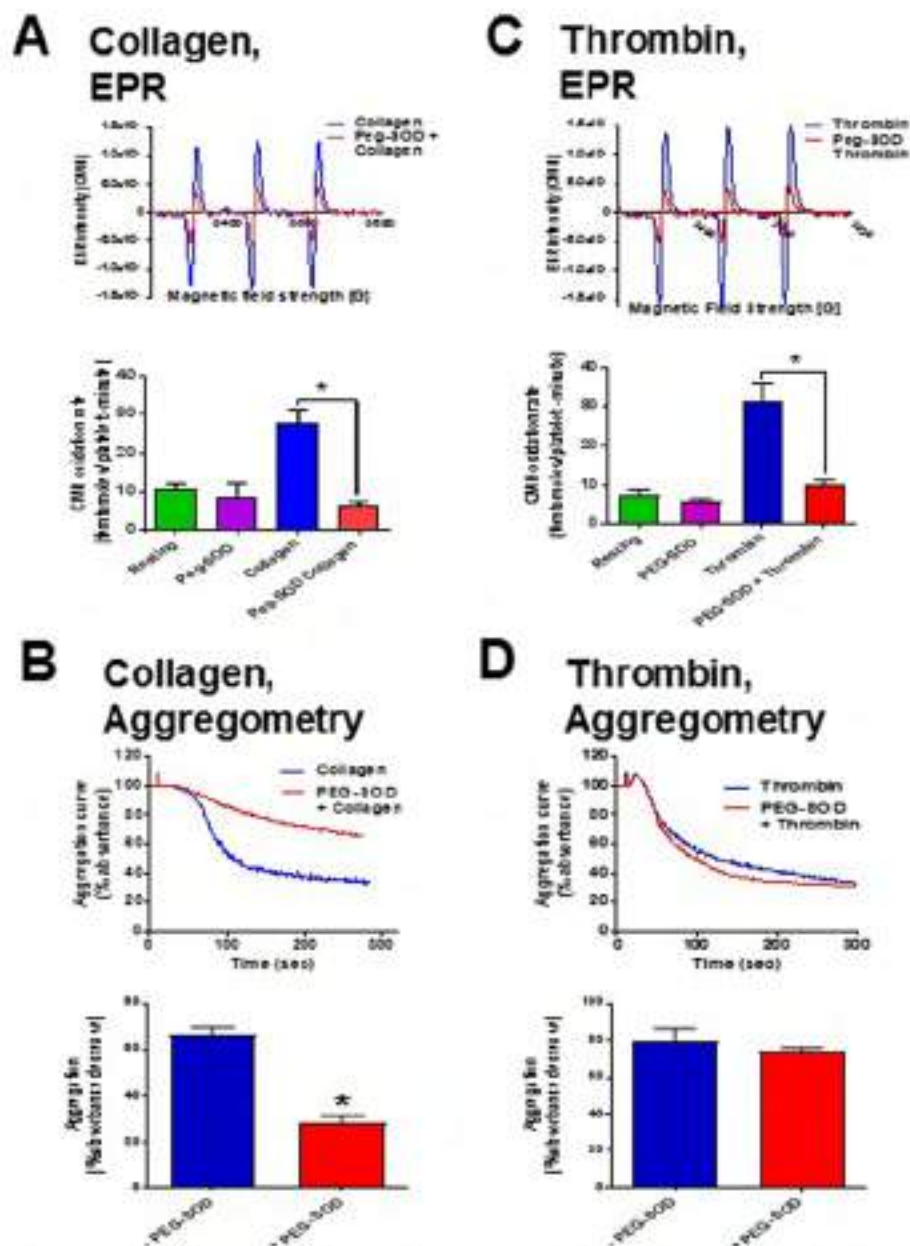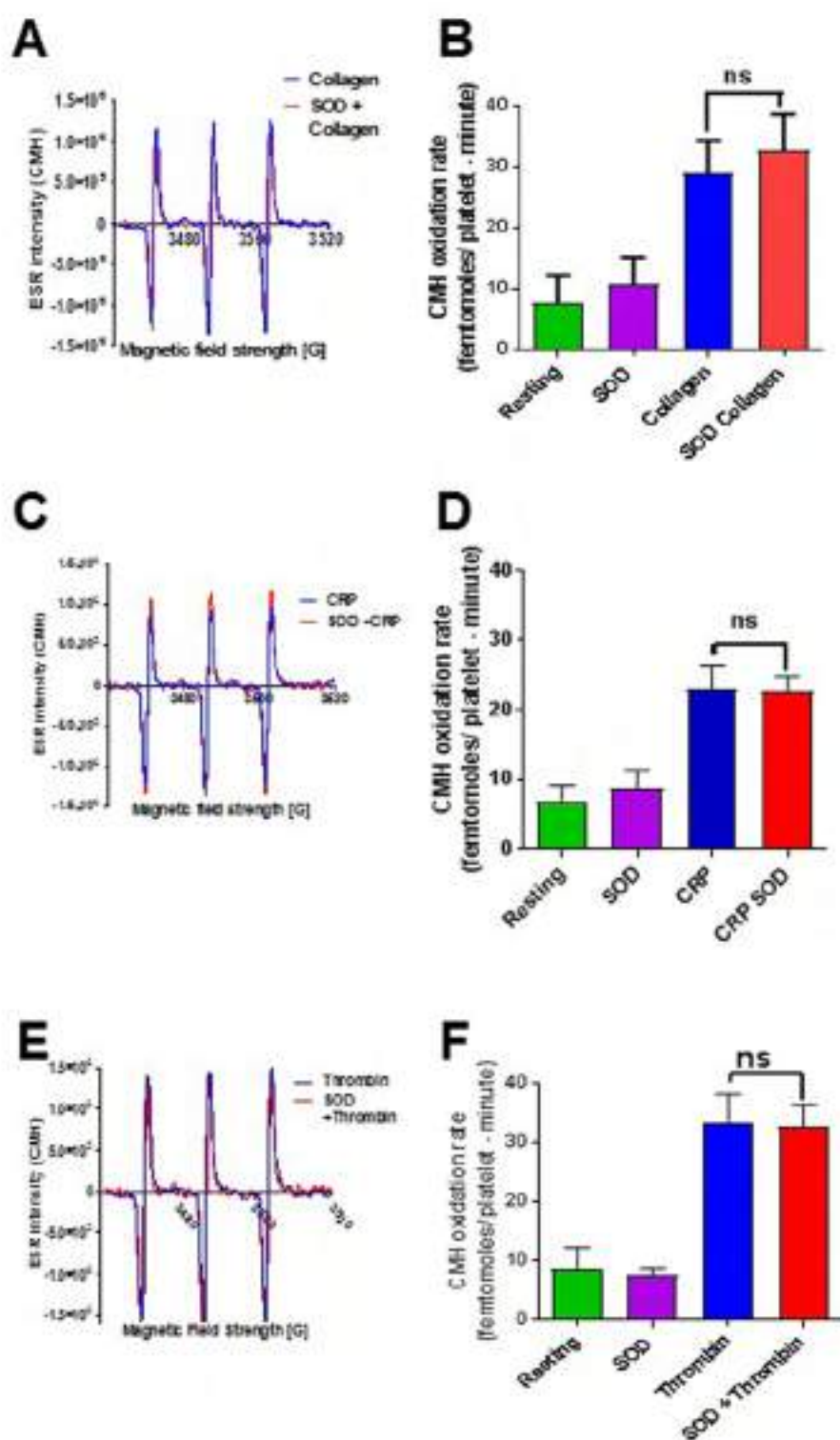
Supplementary Figure 4: Superoxide anions are the oxygen radicals generated in response to collagen and thrombin, and are required only for collagen-dependent aggregation. EPR **(A** and **C)** and aggregation analysis **(B** and **D)** of human platelets stimulated with collagen or thrombin in the presence or absence of 100 unit/ml of PEG-SOD are shown, with representative examples (top) and quantification (bottom). 10 µg/ml collagen or 0.1 unit/ml thrombin were utilised to stimulate platelets. Aggregation curves up to 5 minutes are shown, while EPR resonance readings were taken after 10 minutes of stimulation. Examples of EPR traces and aggregation curves are representative of 4 independent experiments. Statistical analysis was performed by one-way ANOVA with Bonferroni post-hoc test for EPR and by unpaired t-test for aggregation (* = p <0.05, compared to stimulated platelets in the absence of PEG-SOD, n=3 for A and n=4, for B, C and D).
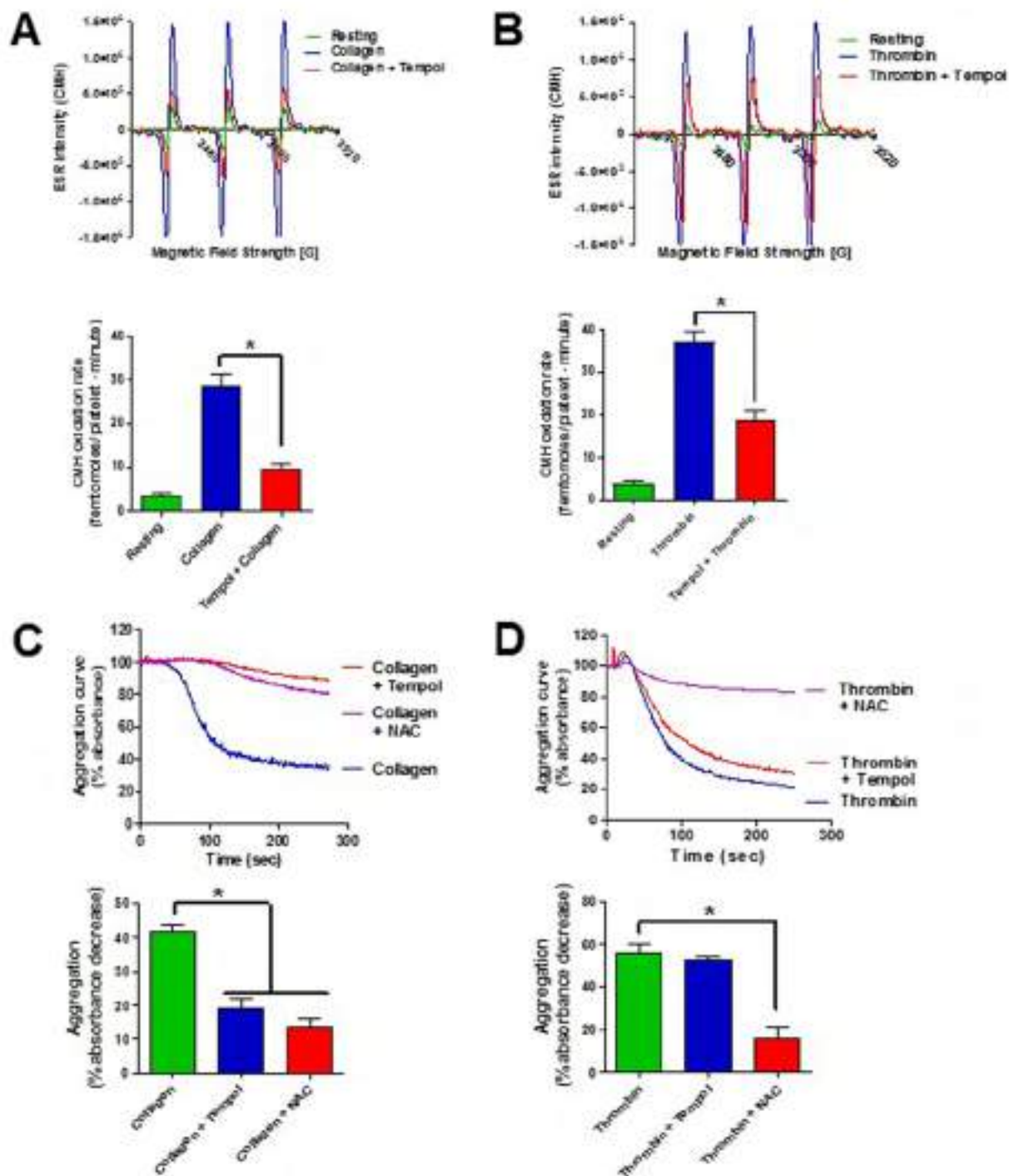
Supplementary Figure 5: Superoxide anions are the oxygen radicals generated in response to collagen and thrombin, but other oxidant species are required for thrombin-stimulated aggregation. . EPR (A and C) and aggregation analysis (B and D) of human platelets stimulated with collagen or thrombin in the presence or absence of 10 µM Tempol are shown, with representative examples (top) and quantification (bottom). 10 µg/ml Collagen or 0.1 unit/ml thrombin were utilised to stimulate platelets. For aggregation experiments, 10mM NAC was also tested. Aggregation curves up to 5 minutes is shown, while EPR resonance readings were taken after 10 minutes of stimulation. Examples of EPR traces and aggregation curves are representative of 3 or more independent experiments. Statistical analysis was performed by one-way ANOVA with Bonferroni post-hoc test for EPR (* = $p < 0.05$, compared to stimulated platelets in the absence of inhibitor) (n=3 for A and C and n=4 for B and D).
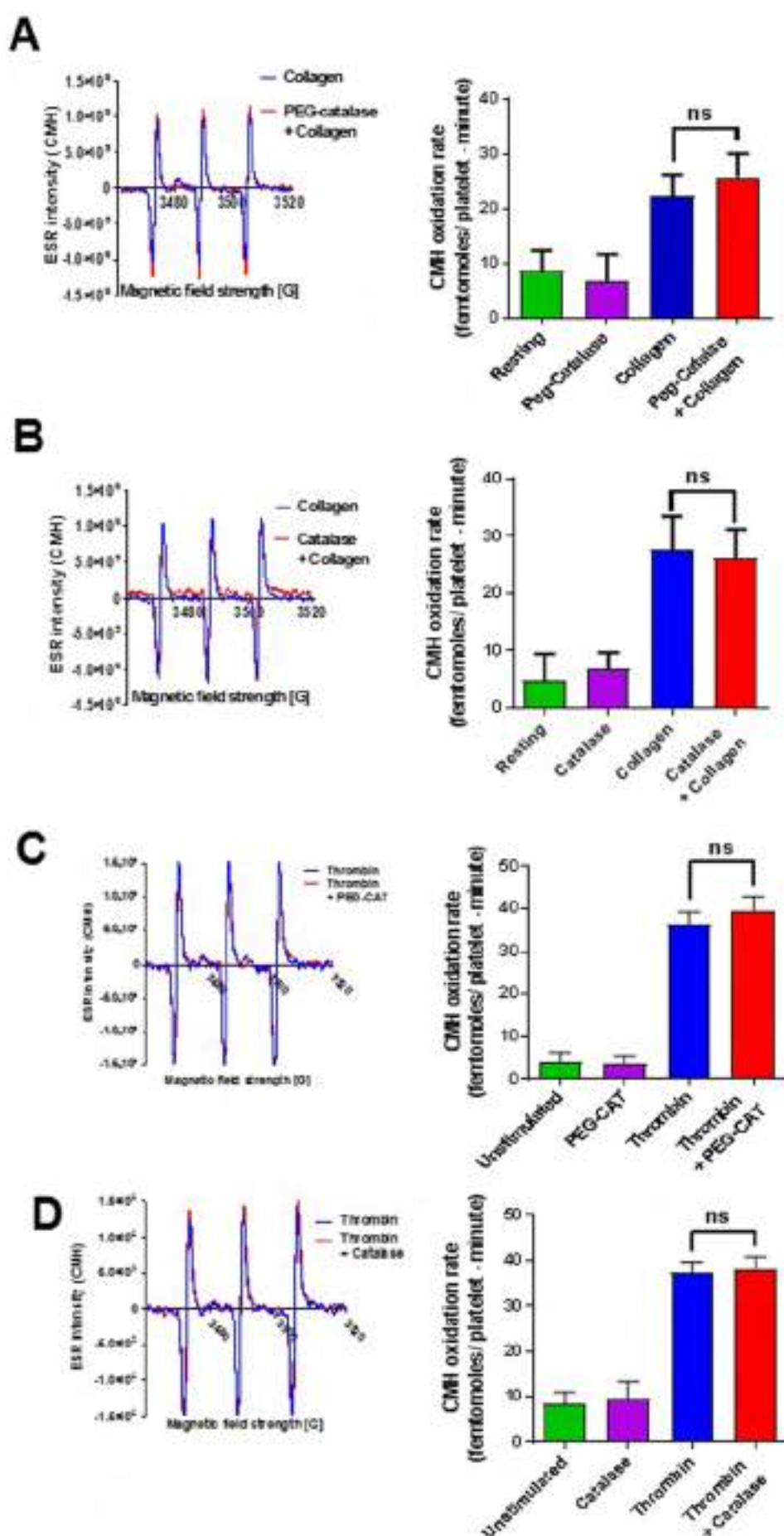
Supplementary Figure 5. Catalase and PEG-Catalase do not affect CMH-based EPR measurement of oxygen radical formation. Human platelets stimulated with collagen (A and B) or thrombin (C and D) in the presence or absence of 500 unit/ml of pegylated catalase (CAT, A and C) or 500 unit/ml catalase (CAT, are shown, with representative examples (left) and quantification (right). 10 μg/ml Collagen or 0.1 unit/ml thrombin were utilised to stimulate platelets. EPR resonance readings were taken after 10 minutes of stimulation. Examples of EPR traces and aggregation curves are representative of 3 independent experiments. Statistical analysis was performed by one-way ANOVA with Bonferroni post-hoc test for EPR (n=3 for A, B, C and D).

Supplementary Figure 7. Superoxide dismutase does not affect CMH-based EPT readings suggesting that only intracellular superoxide anion are detected. Human platelets stimulated with collagen (A and B), CRP (C and D) or thrombin (E and F) in the presence or absence of 100 unit/ml of superoxide dismutase (SOD), with representative examples (A, C and E) and quantification (B, D and F)). 10 µg/ml Collagen, 3 µg/ml CRP or 0.1 unit/ml thrombin were utilised to stimulate platelets. EPR resonance readings were taken after 10 minutes of stimulation. Examples of EPR traces and aggregation curves are representative of 3 or more independent experiments. Statistical analysis was performed by one-way ANOVA with Bonferroni post-hoc test for EPR (n=3 for B and D and n=5 for F).
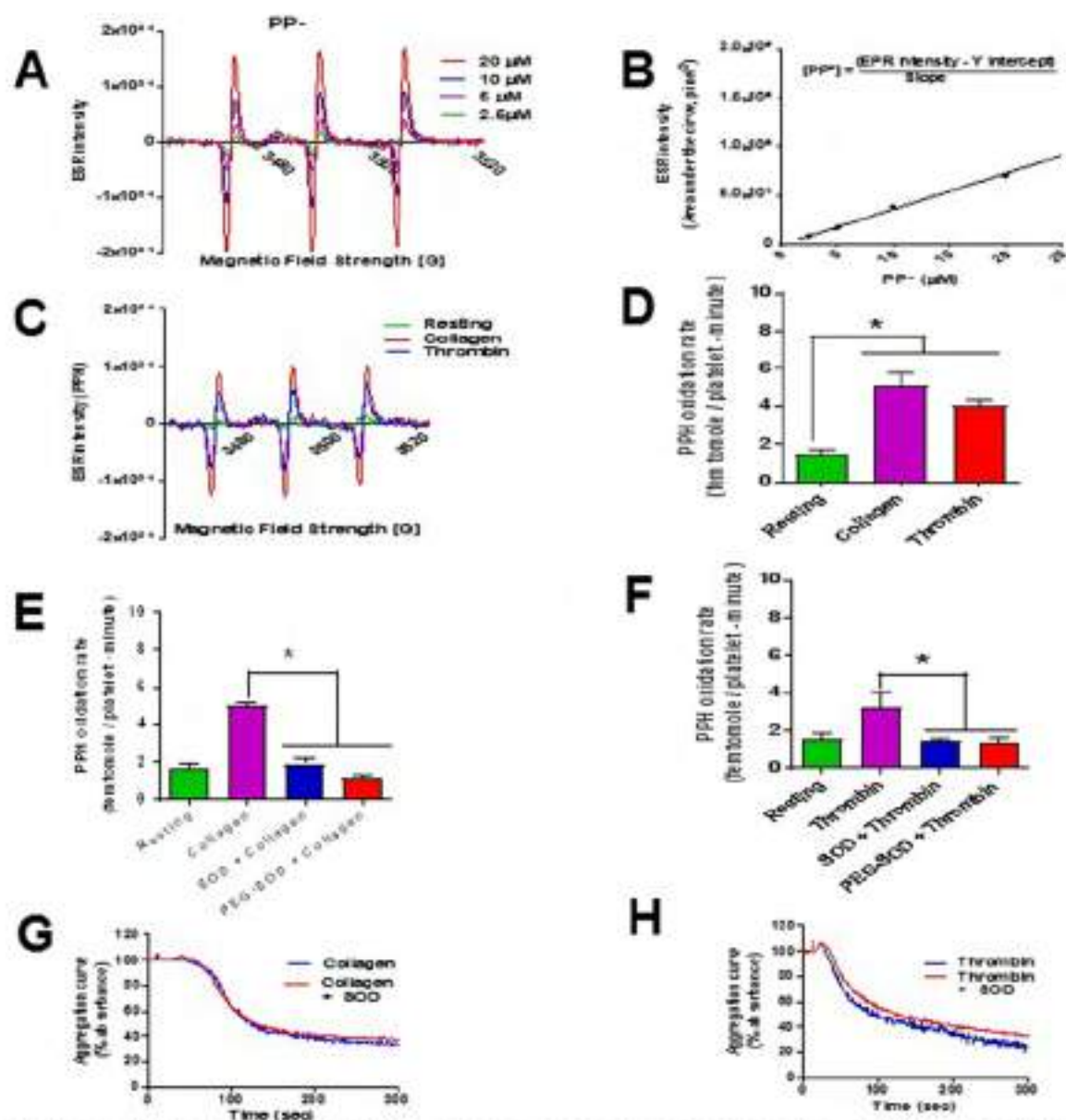
Supplementary Figure 8: Extracellular oxygen radical generation by platelets activated by physiological stimuli collagen and thrombin. PPH was utilised for the detection of extracellular oxygen radicals generated by platelets. A concentration response curve to calibrate the essay for generated (A) and a calibration curve was obtained (B). 10 µg/ml collagen or 0.1 unit/ml thrombin led to generation of extracellular oxygen radicals at low rate (<5 attomoles per platelet per minute) (C and D). 100 unit/ml of PEG-SOD or 100 unit/ml of SOD abolished this response suggesting that extracellular $O_2^{\cdot-}$ were generated (E and F). Interestingly, the scavenging of extracellular $O_2^{\cdot-}$ with SOD did not affect aggregation in response to collagen (G) or thrombin (H). Examples of EPR traces and aggregation curves are representative of 3 or more independent experiments. Statistical analysis was performed by one-way ANOVA with Bonferroni post-hoc test (* = p <0.05, compared to resting platelets, n=3 for F and n=4 for D and E).
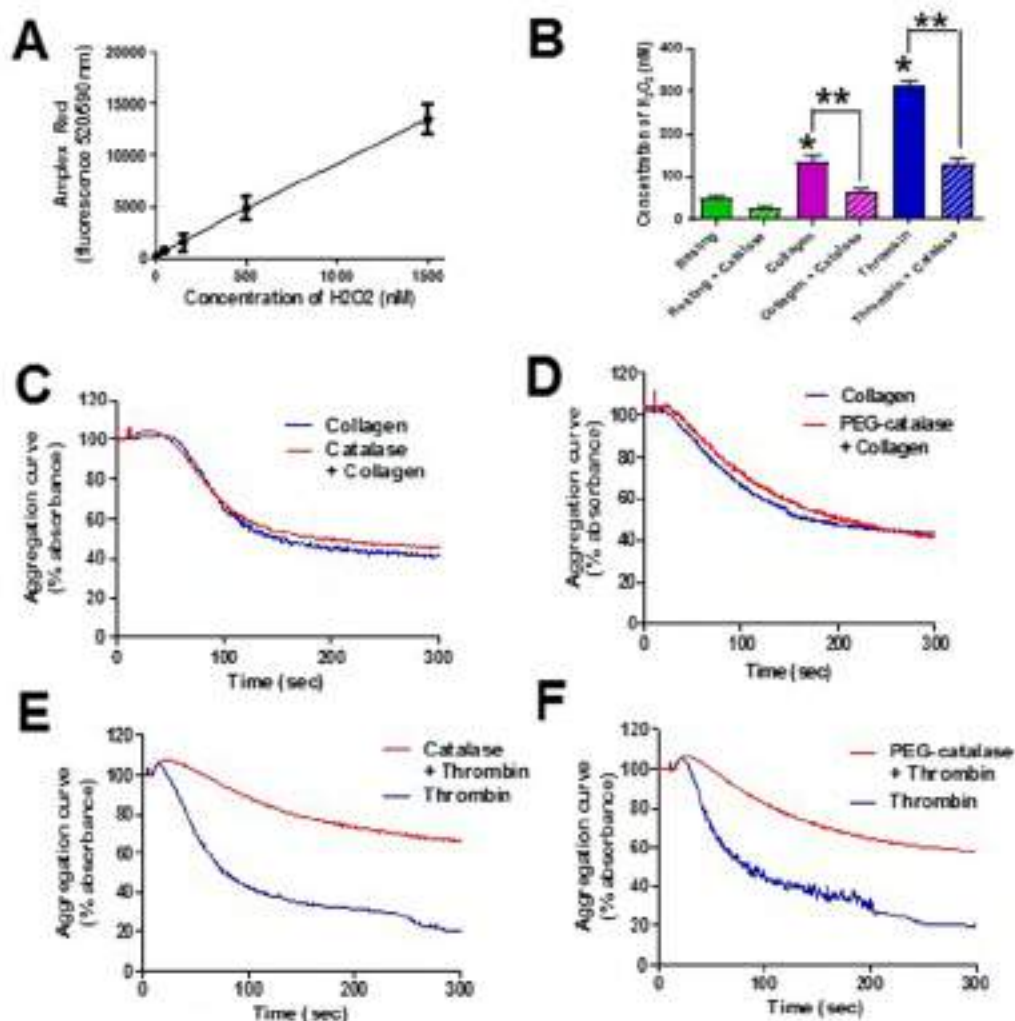
Supplementary Figure 9: Hydrogen peroxide is formed in response to collagen- and thrombin-dependent stimulation of human platelets, but is required only for thrombin-dependent aggregation. A reaction mixture containing 100 µM Amplex Red reagent, and 0.2 U/mL HRP was loaded on black 96 well-plates with or without 100 Units/ml catalase. The reaction was started by adding 50 µl of supernatant obtained from resting and stimulated platelets (2×10^8 platelets/ml). After 30 minutes incubation, the fluorescence (excitation 520 nm, emission 590 nm) was measured using a CLARIOstar microplate reader (BMG LABTECH). In (A) the calibration curve obtained plotting the Amplex Red signal corresponding to different hydrogen peroxide concentrations is shown. The calibration curve was utilised to quantify the hydrogen peroxide released by platelets in resting conditions or in the presence of collagen (10 µg/ml) or thrombin (0.1 unit/ml). Where indicated, 500 unit/ml Catalase were added (as a control) (B). Statistical analysis was performed by one-way ANOVA with Bonferroni post-hoc test for EPR (* = $p < 0.05$, compared to resting platelets, ** = $p < 0.05$ compared to results in the absence of CAT, n=3). Aggregation curves obtained in the same conditions described above are shown in (C-F) and are representative of 3 independent experiments.
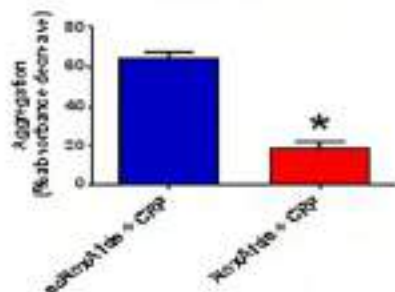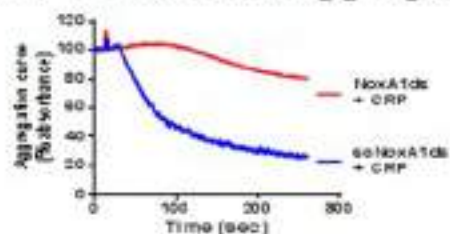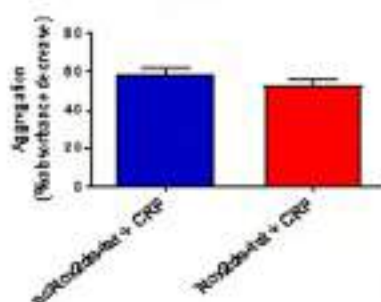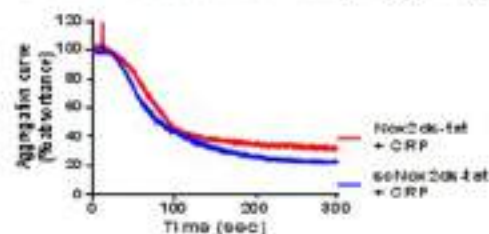
A CRP + NoxA1ds, EPR
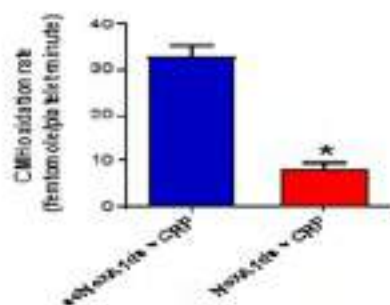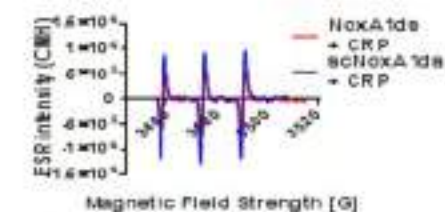

C CRP + Nox2ds-tat, EPR
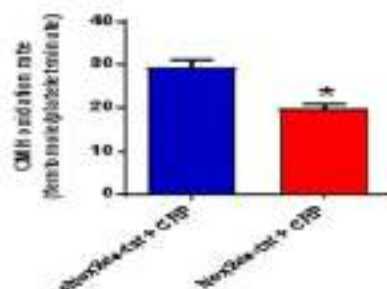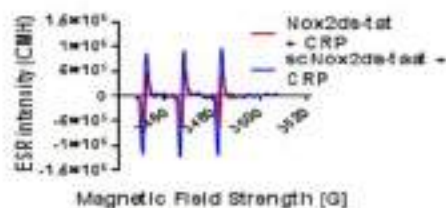

B CRP + NoxA1ds, Aggregometry

D CRP + Nox2ds-tat, Aggregometry

Supplementary Figure 10. CRP-dependent aggregation NOX1- but not NOX2-dependent. Platelet activation was induced with 3 µg/ml CRP oxygen radical generation was assessed by EPR while aggregation was assessed by turbidimetry. 10 µM of NoxA1ds or Nox2ds-tat were utilised to inhibit NOX1 or NOX2, respectively. The scrambled peptide at the same concentration (scNoxA1ds or scNox2ds-tat) were used as a negative control. Examples of EPR traces and aggregation curves are representative of 3 or more independent experiments. Statistical analysis was performed by t-test (* = p <0.05, compared to negative control, i.e. scrambled peptide, n=3 for A and B and n=5 for C and D).
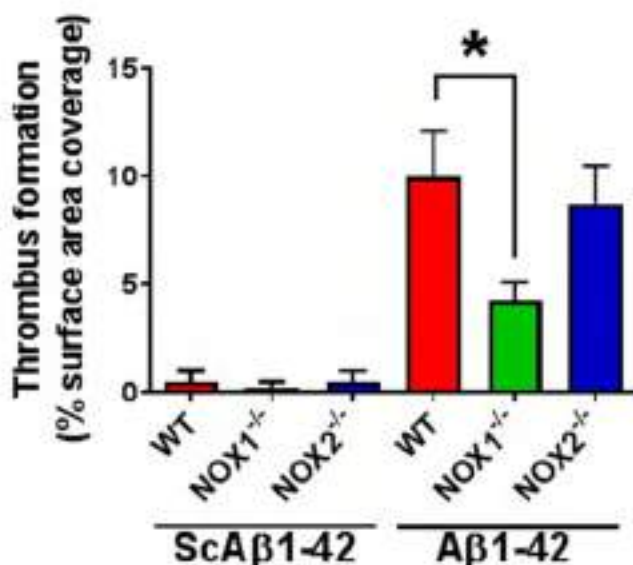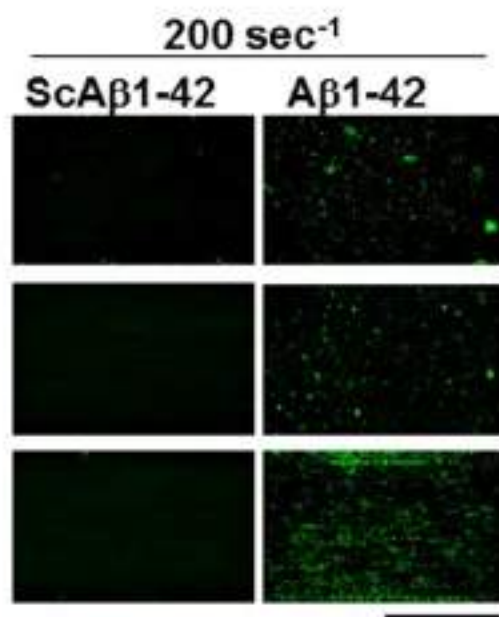
Supplementary Figure 11: Platelet adhesion under low shear stress is NOX1- but not NOX2-dependent. Platelets from wild type, NOX1-/- or NOX2-/- mice were stained with DiOC6 and the Bioflux platform (Fluxion, San Francisco) was utilised to assess the thrombus formation induced by collagen under physiological flow. In A and B, Ibidi Vena8+ flow chambers were coated with 20µM Aβ1-42 or scrambled control peptide (ScAβ1-42). The shear rate utilised was 200 sec^{-1}, which leads to single platelet adhesion. Images were taken at 10 minutes of flow and are representative of 4 independent experiments. They were quantified by assessing the surface area coverage by platelets with Image J. Data are representative of 4 independent experiments. Statistical analysis was performed by one-way ANOVA with Bonferroni post-hoc test (* = $p < 0.05$, n=4).
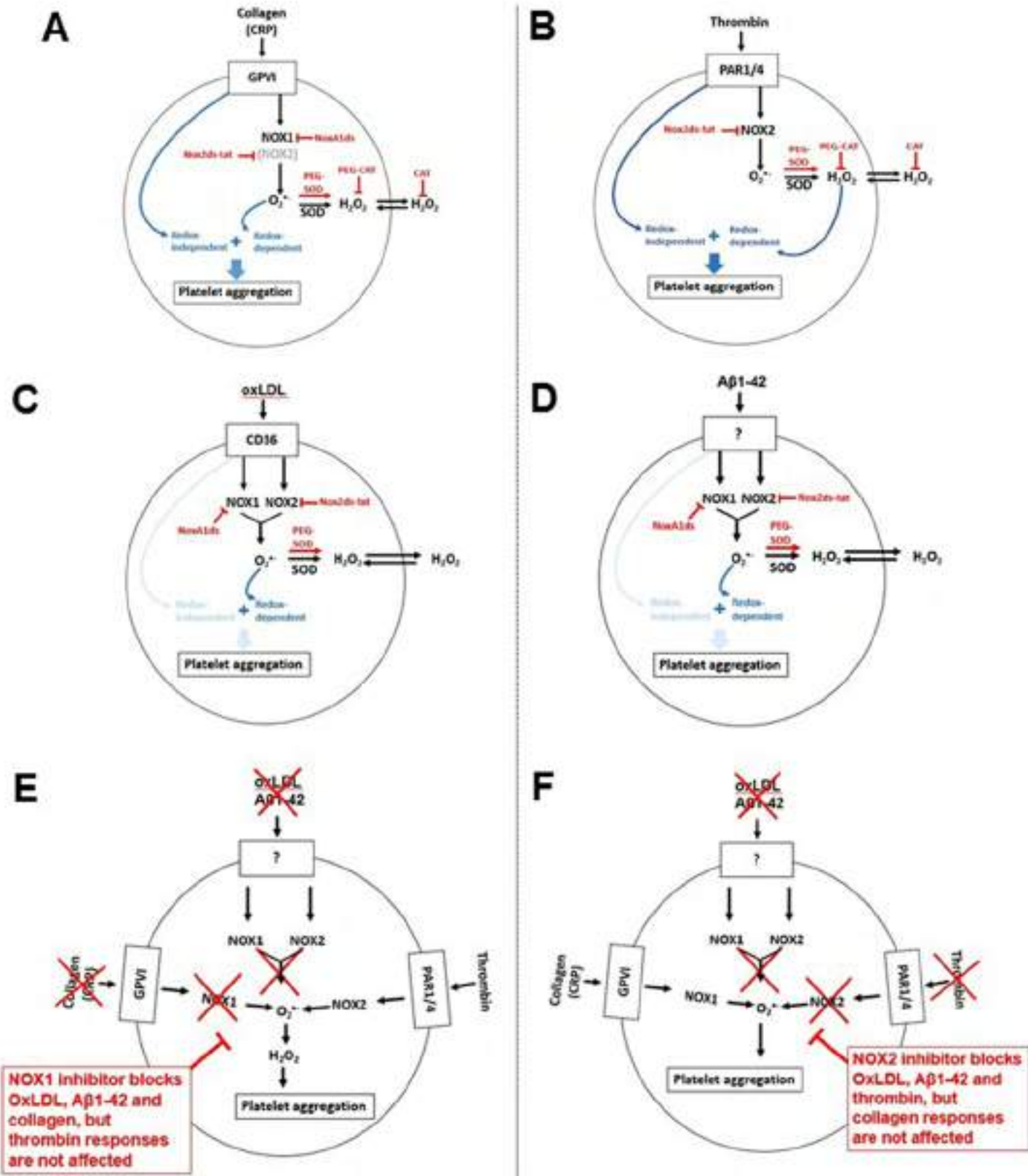
Supplementary Figure 12: Models of the redox-dependence regulation of platelets. The cartoons represent the redox dependence of platelet aggregation in response to collagen (A), thrombin (B), oxLDL (C) or amyloid peptide β 1-42 (D). Selective inhibition of NOX1 would inhibit collagen-, oxLDL- or amyloid peptide β 1-42-dependent response but not thrombin (E), while selective inhibition of NOX2 would inhibit thrombin-, oxLDL- or amyloid peptide β 1-42-dependent response but not collagen (F).

	EPR	Aggregation
Thrombin	0.121 unit/ml	0.088 unit/ml
Collagen	2.63 µg/ml	3.45 µg/ml
CRP	0.77 µg/ml	0.95 µg/ml

Supplemental Table 1: Potency table for different agonists as measured by simultaneous EPR and platelet aggregometry